

Modeling of fission-fragment charge and isotopic distributions.

Peter Möller

Current affiliations: *emeriti Lund University, Consultant MSU*

PRESENTATION LUND,

OCTOBER 31, 2024

Collaborators on this and other projects, see coauthors on papers posted on URL below and publications listed at end.

More details about masses, other projects (beta-decay, fission), associated ASCII data files and figures are at

<http://t2.lanl.gov/nis/molleretal/>

and at list of relevant publications after conclusions.

Stanislav Ulam has remarked:

It is remarkable how a few characters scribbled on a blackboard can change the course of world history.

Feynman:

- I do not care how smart you are
- or how complicated your model is
- If it does not agree with experimental measurements it is wrong!

Letters to the Editor

[The Editor does not hold himself responsible for opinions expressed by his correspondents. Neither can he undertake to return, nor to correspond with the writers of, rejected manuscripts intended for this or any other part of NATURE. No notice is taken of anonymous communications.]

Possible Existence of a Neutron

It has been shown by Bothe and others that beryllium when bombarded by α -particles of polonium emits a radiation of great penetrating power, which has an absorption coefficient in lead of about 0.3 (cm.)^{-1} . Recently Mme. Curie-Joliot and M. Joliot found, when measuring the ionisation produced by this beryllium radiation in a vessel with a thin window, that the ionisation increased when matter containing hydrogen was placed in front of the window. The effect appeared to be due to the ejection of protons with velocities up to a maximum of nearly $3 \times 10^9 \text{ cm. per sec.}$ They suggested that the transference of energy to the proton was by a process similar to the Compton effect, and estimated that the beryllium radiation had a quantum energy of 50×10^6 electron volts.

I have made some experiments using the valve counter to examine the properties of this radiation excited in beryllium. The valve counter consists of a small ionisation chamber connected to an amplifier, and the sudden production of ions by the entry of a particle, such as a proton or α -particle, is recorded by the deflexion of an oscillograph. These experiments have shown that the radiation ejects particles from hydrogen, helium, lithium, beryllium, carbon, air, and argon. The particles ejected from hydrogen behave, as regards range and ionising power, like protons with speeds up to about $3.2 \times 10^9 \text{ cm. per sec.}$ The particles from the other elements have a large ionising power, and appear to be in each case recoil atoms of the elements.

If we ascribe the ejection of the proton to a Compton recoil from a quantum of 52×10^6 electron volts, then the nitrogen recoil atom arising by a similar process should have an energy not greater than about 400,000 volts, should produce not more than about 10,000 ions, and have a range in air at N.T.P. of about 1.3 mm. Actually, some of the recoil atoms in nitrogen produce at least 30,000 ions. In collaboration with Dr. Feather, I have observed the recoil atoms in an expansion chamber, and their range, estimated visually, was sometimes as much as 3 mm. at N.T.P.

These results, and others I have obtained in the course of the work, are very difficult to explain on the assumption that the radiation from beryllium is a quantum radiation, if energy and momentum are to be conserved in the collisions. The difficulties disappear, however, if it be assumed that the radiation consists of particles of mass 1 and charge 0, or neutrons. The capture of the α -particle by the Be^9 nucleus may be supposed to result in the formation of a C^{12} nucleus and the emission of the neutron. From the energy relations of this process the velocity of the neutron emitted in the forward direction may well be about $3 \times 10^9 \text{ cm. per sec.}$ The collisions of this neutron with the atoms through which it passes give rise to the recoil atoms, and the observed energies of the recoil atoms are in fair agreement with this view. Moreover, I have observed that the protons ejected from hydrogen by the radiation emitted in the opposite direction to that of the exciting α -particle appear to have a much smaller range than those ejected by the forward radiation.

This again receives a simple explanation on the neutron hypothesis.

If it be supposed that the radiation consists of quanta, then the capture of the α -particle by the Be^9 nucleus will form a C^{13} nucleus. The mass defect of C^{13} is known with sufficient accuracy to show that the energy of the quantum emitted in this process cannot be greater than about 14×10^6 volts. It is difficult to make such a quantum responsible for the effects observed.

It is to be expected that many of the effects of a neutron in passing through matter should resemble those of a quantum of high energy, and it is not easy to reach the final decision between the two hypotheses. Up to the present, all the evidence is in favour of the neutron, while the quantum hypothesis can only be upheld if the conservation of energy and momentum be relinquished at some point.

J. CHADWICK.

Cavendish Laboratory,
Cambridge, Feb. 17.

The Oldoway Human Skeleton

A LETTER appeared in NATURE of Oct. 24, 1931, signed by Messrs. Leakey, Hopwood, and Reck, in which, among other conclusions, it is stated that "there is no possible doubt that the human skeleton came from Bed No. 2 and not from Bed No. 4". This must be taken to mean that the skeleton is to be considered as a natural deposit in Bed No. 2, which is overlaid by the later beds Nos. 3 and 4, and that all consideration of human interment is ruled out.

If this be true, it is a most unusual occurrence. The skeleton, which is of modern type, with filed teeth, was found completely articulated down even to the phalanges, and in a position of extraordinary contraction. Complete mammalian skeletons of any age are, as field palaeontologists know, of great rarity. When they occur, their perfection can usually be explained as the result of sudden death and immediate covering by volcanic dust. Many of the more or less perfect skeletons which may be seen in museums have been rearticulated from bones found somewhat scattered as the result of death from floods, or in the neighbourhood of drying water-holes. We know of no case of a perfect articulated skeleton being found in company with such broken and scattered remains as appear to be abundant at Oldoway. Either the skeletons are all complete, as in the *Stenomylus* quarry at Sioux City, Nebraska, or are all scattered and broken in various degrees, as in ordinary bone beds. The probability, therefore, that the Oldoway skeleton represents an artificial burial is thus one that will occur to palaeontologists.

The skeleton was exhumed in 1913, and published photographs show that the excavation made for its disinterment was extensive. It is, therefore, very difficult to believe that in 1931 there can be reliable evidence left at the site as to the conditions under which it was deposited. If naturally deposited in Bed No. 2, the skeleton is of the highest possible importance, because it would be of pre-Mousterian age, and would be in the company of *Pithecanthropus* and the Piltdown, Heidelberg, and Peking men, all of whose remains are fragmentary to the last degree. Of the few other human remains for which such antiquity is claimed, the Galley Hill skeleton and the Ipswich skeleton are, or apparently were, complete. The first of these was never seen *in situ* by any trained observer, and the latter has, we believe, been withdrawn by its discoverer. The other fragments, found long ago, are entirely without satisfactory evidence as to their mode of occurrence.

Nuclear **BINDING ENERGY**

Bethe-Bacher (-Weizäcker) (1936)

$$B(N, Z) =$$

$$+a_V A \quad (\text{Volume energy})$$

$$-a_S A^{2/3} \quad (\text{Surface energy})$$

$$-a_C \frac{Z^2}{A^{1/3}} \quad (\text{Coulomb energy})$$

$$-a_I \frac{(N - Z)^2}{A} \quad (\text{Symmetry energy})$$

$$-\delta(A) \quad (\text{Pairing energy})$$

Bethe and Bacher, Revs. Mod. Phys. **8** (1936) 82

Bethe and Bacher,
Revs. Mod. Phys. **8** (1936) 82 (in §33):

“There remains thus the nucleus containing 8 neutrons and 8 protons, i.e. , ^{16}O , to test the shell structure” hypothesis by means of nuclear energies. It seems in fact that there is ample evidence for a particular stability of ^{16}O , and thus for the individual-particle approximation.”

So, already in 1936, shell-structure, single-particle models, and how they might modify a macroscopic model were in mainstream discussions.

Hahn and Strassman conclusively identified barium in the products after bombarding uranium with neutrons

(Naturwiss. **27** (1939) 11)

Meitner and Frisch proposed that observations of barium in the reaction products were due to nucleus deforming like a drop

(Nature **143** (1939) 239)

Frisch measured (the predicted) fragment high kinetic energies

(Nature **143** (1939) 239)

Bohr and Wheeler Calculated

(Phys. Rev. **56** (1939) 426):

**Nuclear POTENTIAL ENERGY
versus deformation**

$$B(N, Z) =$$

$$+a_V A \quad (\text{Volume energy})$$

$$-a_S A^{2/3} B_S(\beta) \quad (\text{Surface energy})$$

$$-a_C \frac{Z^2}{A^{1/3}} B_C(\beta) \quad (\text{Coulomb energy})$$

$$-a_I \frac{(N - Z)^2}{A} \quad (\text{Symmetry energy})$$

$$-\delta(A) \quad (\text{Pairing energy})$$

Nuclear Deformation Energy

Let the nuclear surface be described by

$$r(\theta, \phi) = R_0 [1 + \alpha_2 P_2(\cos \theta)]$$

The surface energy lowest order Taylor expansion:

$$E_s = E_s^0 \left(1 + \frac{2}{5} \alpha_2^2\right)$$

The Coulomb energy lowest order Taylor expansion

$$E_C = E_C^0 \left(1 - \frac{1}{5} \alpha_2^2\right)$$

The energy at deformation α_2 relative to spherical shape

$$E_{\text{def}}(\alpha_2) = E_C(\alpha_2) + E_s(\alpha_2) - (E_C^0 + E_s^0)$$

If E_{def} is negative then the system has no barrier wrt fission

$$E_{\text{def}}(\alpha_2) = \frac{2}{5} \alpha_2^2 E_s^0 - \frac{1}{5} \alpha_2^2 E_C^0 < 0$$

$$1 < \frac{E_C^0}{2E_s^0} = x$$

The surface energy for a sphere

$$E_s^0 = 17.80A^{2/3}$$

The Coulomb energy for a sphere

$$E_C^0 = 0.7103 \frac{Z^2}{A^{1/3}}$$

The fissility parameter x :

$$x = \frac{Z^2}{50.13A}$$

Z	A	x
50	124	0.402
82	208	0.645
92	138	0.709
100	252	0.792
114	298	0.870
125	328	0.950
130	335	1.006

Swiatecki (and others) observed that experimental actinide spontaneous-fission half-lives differed substantially from what could be explained from smoothly varying (with neutron number and proton number) liquid drop barriers.

He correlated the differences with differences between liquid-drop ground state masses and measured masses and found that such ground-state “shell structure” could account for the observed behavior of actinide spontaneous fission half-lives.

trend is consistent with a straight line, defining $(Z^2/A)_e = 40.2 \pm 0.7$. The equation of the line leads to the semiempirical formula,

$$M_2 - M_1 = 0.090(40.2 \pm 0.7 - Z^2/A)^{1/2}A. \quad (4)$$

One may combine Eq. (4) with the relation:

$$M_2 + M_1 = A - \nu$$

(ν = number of neutrons emitted in fission),

to predict the positions of the peaks in the yield curves of elements that have not yet been investigated. If an average value $\bar{\nu} = 2.8$ is used, one finds

$$M_2 = \frac{1}{2}A - 1.4 + 0.045(40.2 \pm 0.7 - Z^2/A)^{1/2}A, \quad (5)$$

$$M_1 = \frac{1}{2}A - 1.4 - 0.045(40.2 \pm 0.7 - Z^2/A)^{1/2}A. \quad (6)$$

The present analysis provides a reason for the empirical observation that in the fission of different elements the position of the heavy peak remains

TABLE I. Positions of the peaks in the fission yield curves.

Compound nucleus	Position of peaks				Remarks	Reference
	Observed ^a	M_1	Formulas (5), (6)			
	M_2	M_1	M_2	M_1		
Th ²³³	140	91	139.1	91.1	Low-energy neutron fission	b
U ²³⁹	140	98	141.1	95.1		c
U ²³⁶	138.5	95	138.2	95.0		d
U ²³⁴	137	93	136.2	95.0		b, e
Pu ²⁴⁰	138	99	137.9	99.3		c
U ²³⁸	140	96	140.2	95.0	Spontaneous fission	f, g
Cm ²⁴²	136	103	134.7	104.5		g
Cf ²⁵²	139	108	140.2	109.0		h

^a The uncertainty in the observed values of M_2 and M_1 is of the order of ± 1 or ± 2 mass units. (It is more in the cases of U²³⁹ and U²³⁸.) No systematic attempt has been made to adjust $A - M_2 - M_1$ to agree with available information on the number of emitted neutrons.

^b A. Turkevich and J. B. Niday, Phys. Rev. **84**, 52 (1951).
^c E. B. Steinberg and M. S. Freedman, *Radiochemical Studies: The Fission Products* (McGraw-Hill Book Company, Inc., New York, 1951), Paper No. 219, National Nuclear Energy Series, Plutonium Project Record, Vol. 9, Div. IV, Part V.

^d Glendenin, Steinberg, Ingraham, and Hess, Phys. Rev. **84**, 860 (1951).

^e Steinberg, Glendenin, Ingraham, and Hayden, Phys. Rev. **95**, 867 (1954).

^f G. W. Wetherill, Phys. Rev. **92**, 907 (1953).

^g E. P. Steinberg and L. E. Glendenin, Phys. Rev. **95**, 431 (1954).

^h E. P. Steinberg and L. E. Glendenin, J. Inorg. Nuc. Chem. **1**, 45 (1955).

approximately constant. If the degree of asymmetry remained unchanged from nucleus to nucleus, both peaks would move towards higher masses with increasing A . In fact, there is superimposed on this shift a coming together of the peaks with increasing Z^2/A . Since the over-all trend of Z^2/A is to increase with A , the result is that for the light peak the two shifts add up whereas for the heavy peak they partly cancel. This is illustrated in Table I, where M_2 and M_1 , calculated according to (5) and (6), are compared with the observed values.

Further measurements of fission asymmetries would be interesting, especially in the region of Z^2/A close to the critical value, where the present considerations suggest a rapid decrease of $M_2 - M_1$.

It is a pleasure to acknowledge stimulating discussions with Professor S. G. Thompson, Dr. A. C. Pappas, and Dr. T. Maris.

¹ N. Bohr and J. A. Wheeler, Phys. Rev. **56**, 426 (1939).

² A. E. S. Green, Phys. Rev. **95**, 1006 (1954).

³ W. J. Swiatecki (to be published).

⁴ D. L. Hill and J. A. Wheeler, Phys. Rev. **89**, 1102 (1953).

Systematics of Spontaneous Fission Half-Lives

W. J. SWIATECKI

Institute for Mechanics and Mathematical Physics and The Gustaf Werner Institute for Nuclear Chemistry, Uppsala, Sweden

(Received July 18, 1955)

SEVERAL authors have noted the over-all trend of spontaneous fission half-lives to decrease with increasing Z^2/A as well as the considerable deviations (by several powers of 10) from any smooth dependence on this parameter.¹ We should like to discuss the close correlation which seems to exist between the half-lives and the finer details in the systematics of the ground-state masses of nuclei.²

A simple way of exhibiting this correlation is to plot the deviation $\delta\tau$ from a straight line in a plot of τ [$\tau = \log_{10}(\text{half-life})$] vs Z^2/A , against deviations (δM) of the masses M of the nuclei from a smooth reference surface $M_{\text{ref}}(A, Z)$. We made such a plot, with M_{ref} taken to be the semiempirical mass surface of Green³ (based on the liquid drop model):

$$\begin{aligned} \delta M &= M - M_{\text{ref}}, \\ M_{\text{ref}} &= 1000A - 8.3557A + 19.120A^{\frac{2}{3}} \\ &\quad + 0.76278Z^2/A^{\frac{1}{3}} + 25.444(N - Z)^2/A \\ &\quad + 0.420(N - Z) \text{ millimass units.} \quad (1) \end{aligned}$$

The experimental masses M were taken from Glass *et al.*⁴

In the case of even-even nuclei the plot of $\delta\tau$ vs δM suggested a series of straight lines, one for each Z , indicating that for the isotopes of one element special stability of a nucleus (small δM) is invariably associated with a longer lifetime (large $\delta\tau$). The lines had approximately the same slope, thus defining a spontaneous-fission hindrance factor which corresponds to about 10^6 times longer lifetime for each millimass unit of extra stability. This suggested that if the observed lifetimes were corrected for the variations in stability of the ground states, a more regular dependence of τ on Z^2/A might be discernible.

Figure 1 shows the effect on the plot of τ vs Z^2/A of adding to the observed τ_{exp} an empirical correction $k\delta M$ ($k \sim 5$ if δM in mMU). For even-even nuclei the values of $\tau_{\text{exp}} + k\delta M$ define a fairly smooth curve, with indications of a similar curve for odd- A nuclei. [In a

preliminary plot the hindrance factor k was taken to be 5. A small but significant further smoothing of the points resulted from making k vary with Z^2/A according to $k=5-(Z^2/A-37.5)$. This is the case shown in Fig. 1.]

The result can be stated in the form of an empirical formula for half-lives; e.g., for even-even nuclei,

$$\tau_{ee} = f(Z^2/A) - k\delta M, \quad (2)$$

where f is the curve defined by the even-even points in Fig. 1. The relation of the points for odd- A nuclei to the curve obtained from (2) by a shift upwards of 6.6 units is also shown in Fig. 1. The lifetime of the odd-odd nucleus E^{254} (einsteinium, $Z=99$) is consistent with a further shift of 4.9 units. The curve $f(Z^2/A)$ can be

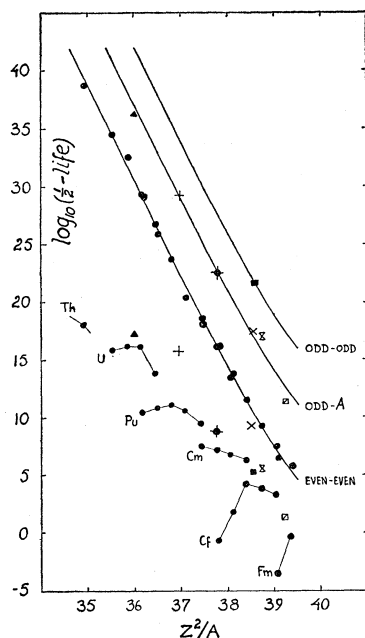


FIG. 1. Plot of spontaneous fission half-lives against Z^2/A . The observed lifetimes τ_{exp} occupy the bottom left-hand part of the figure; the "corrected" values $\tau_{\text{exp}} + k\delta M$ group themselves around the three curves. Experimental points for even-even nuclei are joined by straight lines. Odd- A nuclei are designated by special symbols which, reading from left to right along the odd- A curve, refer to U^{235} , Pu^{239} , Bk^{249} , Cf^{249} , E^{253} (einsteinium, $Z=99$), and Fm^{255} (fermium, $Z=100$). The odd-odd nucleus E^{254} is marked by a square.

represented for example by a cubic, which leads to the following formulas for the lifetimes:

$$\left. \begin{array}{l} \tau_{ee} = 18.2 \\ \tau_{\text{odd } A} = 24.8 \\ \tau_{oo} = 29.7 \end{array} \right\} - 7.8\theta + 0.35\theta^2 + 0.073\theta^3 - (5-\theta)\delta M, \quad (3)$$

where $\theta = (Z^2/A) - 37.5$, and δM is the deviation in mMU of the experimental mass from the surface (1). Table I compares the observed half-lives with the values calculated by means of (3). The remarkable

TABLE I. Values of $\log_{10}(\text{half-life})$.

Nucleus	Experi- mental ^a	Formula (3)	Nucleus	Experi- mental ^a	Formula (3)
Even-even nuclei			Even-even nuclei		
Th 230	≥ 7.18	19.39	Cf 246	3.32	3.27
232	18.15	18.84	248	3.85	3.92
U 232	13.90	13.56	250	4.18	4.24
234	16.30	15.98	252	1.82	1.60
236	16.30	15.21	254	-0.70	-1.02
238	15.90	15.52	Fm 254	-0.30	-0.85
Pu 236	9.54	9.66	256	-3.52	-3.02
238	10.69	11.57	Odd- A nuclei		
240	11.08	11.09	U 235	17.26?	18.02
242	10.86	11.22	Pu 239	15.74	15.42
244	10.40	10.13	Bk 249	8.78	8.67
Cm 244	6.28	6.27	Cf 249	9.18	8.65
242	6.86	7.27	E 253	5.48	4.38
244	7.15	7.09	Fm 255	1.30	2.79
246	7.48	7.88	Odd-odd nuclei		
			E 254	5.18	5.17

^a The experimental values are from a summary by A. Ghiorso, kindly lent to me by Professor S. G. Thompson.

degree of smoothing achieved by means of the unsophisticated correction $k\delta M$ is illustrated by the fact that the deviations from (3) rarely exceed 0.5. (Note that a shift in τ of this amount would be produced by an error of 0.1 mMU in δM .)

The importance of shell structure in the fission process is suggested by the fact that, according to the present considerations, the oscillations of the masses (associated with individual particle structure) in the range $\delta M = 1-3$ mMU shorten the lifetimes by factors of 10^5 to 10^{15} . On the other hand the irregularities in the original plot of τ_{exp} against Z^2/A are seen to be largely due to irregularities in the ground-state masses, associated with *shell structure in the ground-state configuration*. The smoothness of the points $\tau_{\text{exp}} + k\delta M$ suggests that, after correcting for shell structure in the ground-state configuration, the description of the fission process in terms of a model in which single-particle features are treated in an average way may be useful. Qualitative reasons for the greater validity of such an averaged description for the more strongly deformed nuclear shapes occurring in fission may be found in the disappearance for such shapes of degeneracies in the energy spectrum associated with the proximity to a spherically symmetric configuration.

It is a pleasure to acknowledge discussions with Professor S. G. Thompson and Dr. A. C. Pappas and stimulating contacts with Dr. Aage Bohr and Dr. B. R. Mottelson and members of the C.E.R.N. Theoretical Study Group in Copenhagen.

¹ See for example J. R. Huizenga, Phys. Rev. **94**, 158 (1954).

² The existence of correlations between nuclear masses, fission thresholds, and half-lives has been considered by Professor D. Frisch, to whom I am greatly indebted for stimulating discussions.

³ A. E. S. Green, Phys. Rev. **95**, 1006 (1954).

⁴ Glass, Thompson, and Seaborg, J. Inorg. Nuc. Chem. **1**, 3 (1955).

CERN 55 - 30

THEORETICAL STUDY DIVISION

Det Kongelige Danske Videnskabernes Selskab

Matematisk-fysiske Meddelelser, bind 29, nr 16

Dan Mat Fys Medd 29, no 16 (1955)

BINDING STATES
OF INDIVIDUAL NUCLEONS IN
STRONGLY DEFORMED NUCLEI

BY

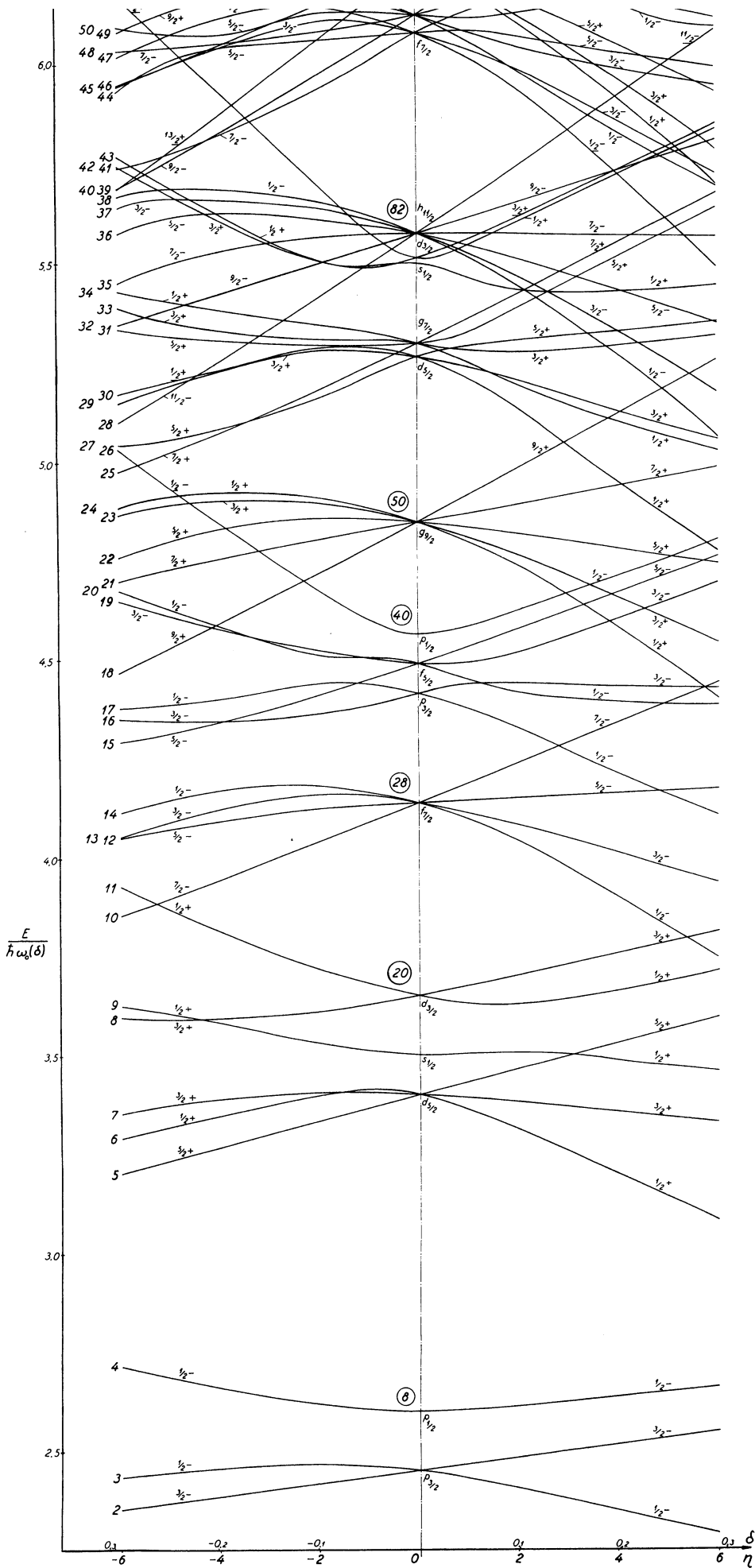
SVEN GÖSTA NILSSON

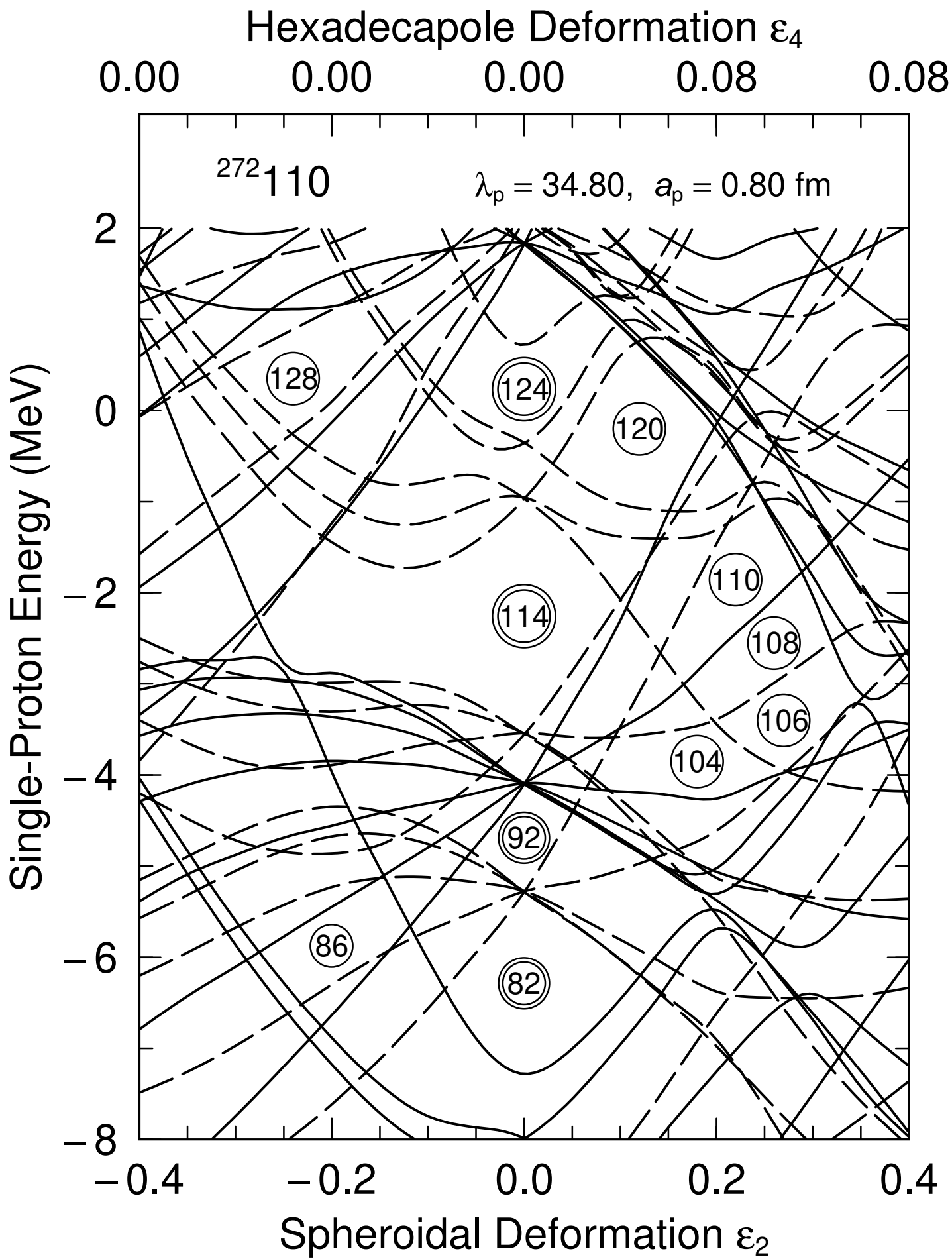


København 1955

i kommission hos Ejnar Munksgaard

There is a scale for both of the deformation variables η and δ . To first order δ equals the deformation parameter β used in the papers of A. Bohr and B. Mottelson. The energy is plotted in the A - and δ -dependent energy unit $\pi h \omega_0(\delta)$, where $h \omega_0$ varies with A as $A^{-1/3}$. Further, for $A \approx 100$ one expects $h \omega_0 \approx 8.8$ MeV. The constant π is chosen equal to 0.05 in the diagram. The levels are labelled by the J^π -number and the parity. The numbers to the left of the curves refer to Table I.





1.D.4:
1.E.2

Nuclear Physics A95 (1967) 420—442; © North-Holland Publishing Co., Amsterdam
Not to be reproduced by photoprint or microfilm without written permission from the publisher

SHELL EFFECTS IN NUCLEAR MASSES AND DEFORMATION ENERGIES

V. M. STRUTINSKY

*I. V. Kurchatov Institute of Atomic Energy
Moscow, USSR*

Received 20 October 1966

Abstract: Nuclear shells correspond to an inhomogeneous distribution of nucleons in phase space, whereas the distribution in quasi-classical phenomenological models (the liquid drop model) is supposed to be homogeneous. Starting from this point, Nilsson's level scheme is used to calculate the shell-model correction to the "liquid drop energy" of the nucleus as a function of the occupation number and deformation. A strong correlation between the shell correction and nucleon level density at the Fermi energy was observed. In magic and mid-shell nuclei the calculated deformation energy oscillates around the LDM value. Discussion of problems related to the deformation energy such as nuclear deformations, shell effects in nuclear masses, in deformed nuclei and in nuclear fission, etc. is presented. The role of nucleon pairing is discussed.

1. Introduction

The problem of nuclear masses and their dependence on deformation is one of the oldest in nuclear theory. There are several approaches to the problem, one of which is the so-called liquid drop model (LDM), which is commonly used in the description of nuclear masses and in nuclear fission theories. The LDM is based on the assumption of a classically uniform distribution of nucleons in phase space and thus ignores completely nucleon shell effects. The importance of such (quantum) effects is stressed however in the Bohr-Mottelson unified model. In more microscopic models, an attempt is made to reduce the problem to residual nucleon interactions, e.g. quadrupole-quadrupole and pairing interactions.

A completely quantitative microscopic description of nuclear deformations is hardly possible at present. Modern theories of nuclear excitations use a renormalized Hamiltonian and assume that the properties of the average field are known from empirical data. The problem of nuclear masses and deformations is complicated by the necessity of calculating the average field and the energy related to it and some other quantities such as the surface tension constant. In the surface region the nucleon density decreases to zero in a very short distance of the order of $A^{-\frac{1}{3}}R_0$, i.e. a large density gradient is present. The problem of surface tension arises for which features of nucleon interactions such as saturation (velocity dependence) are important.

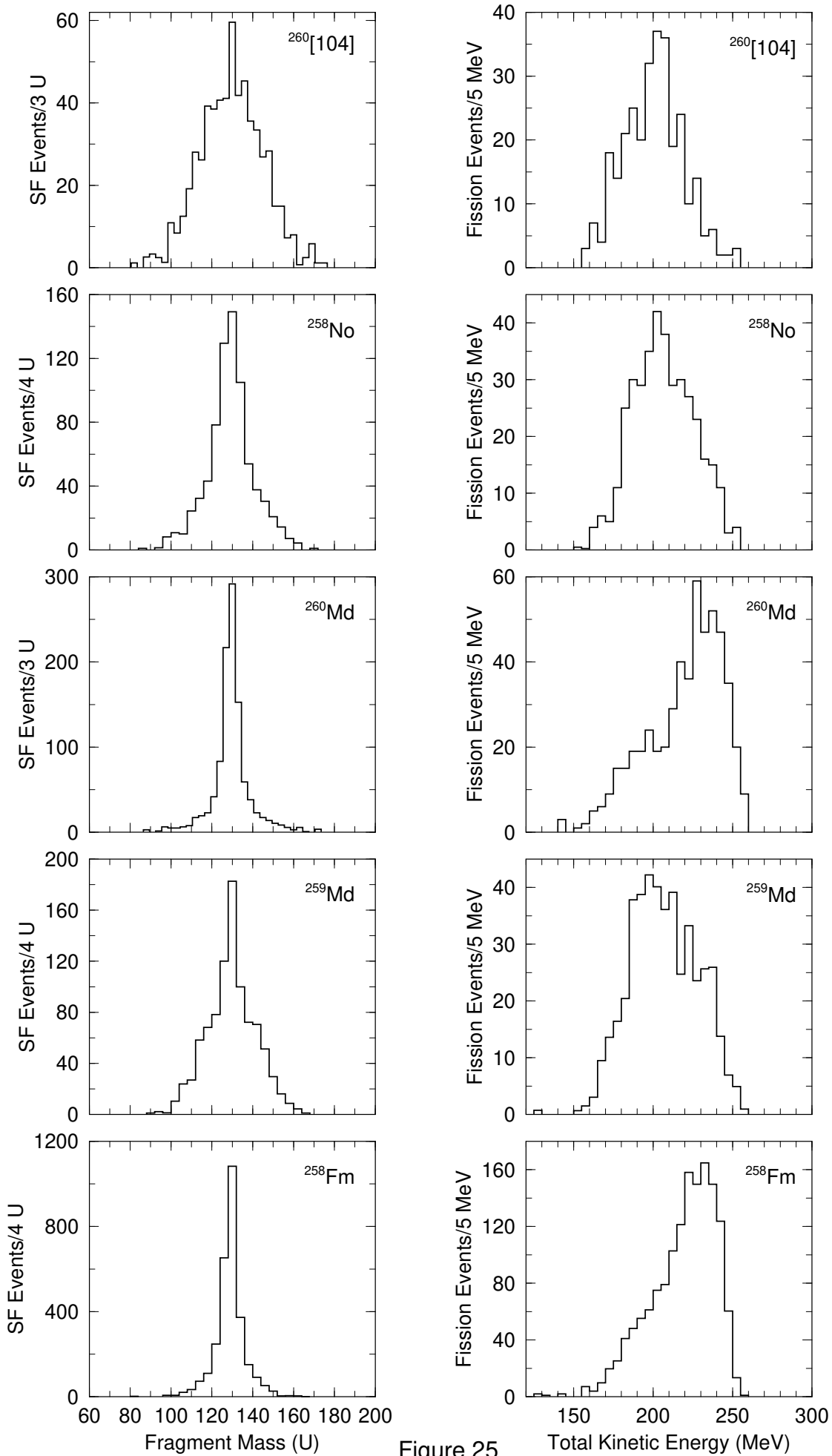
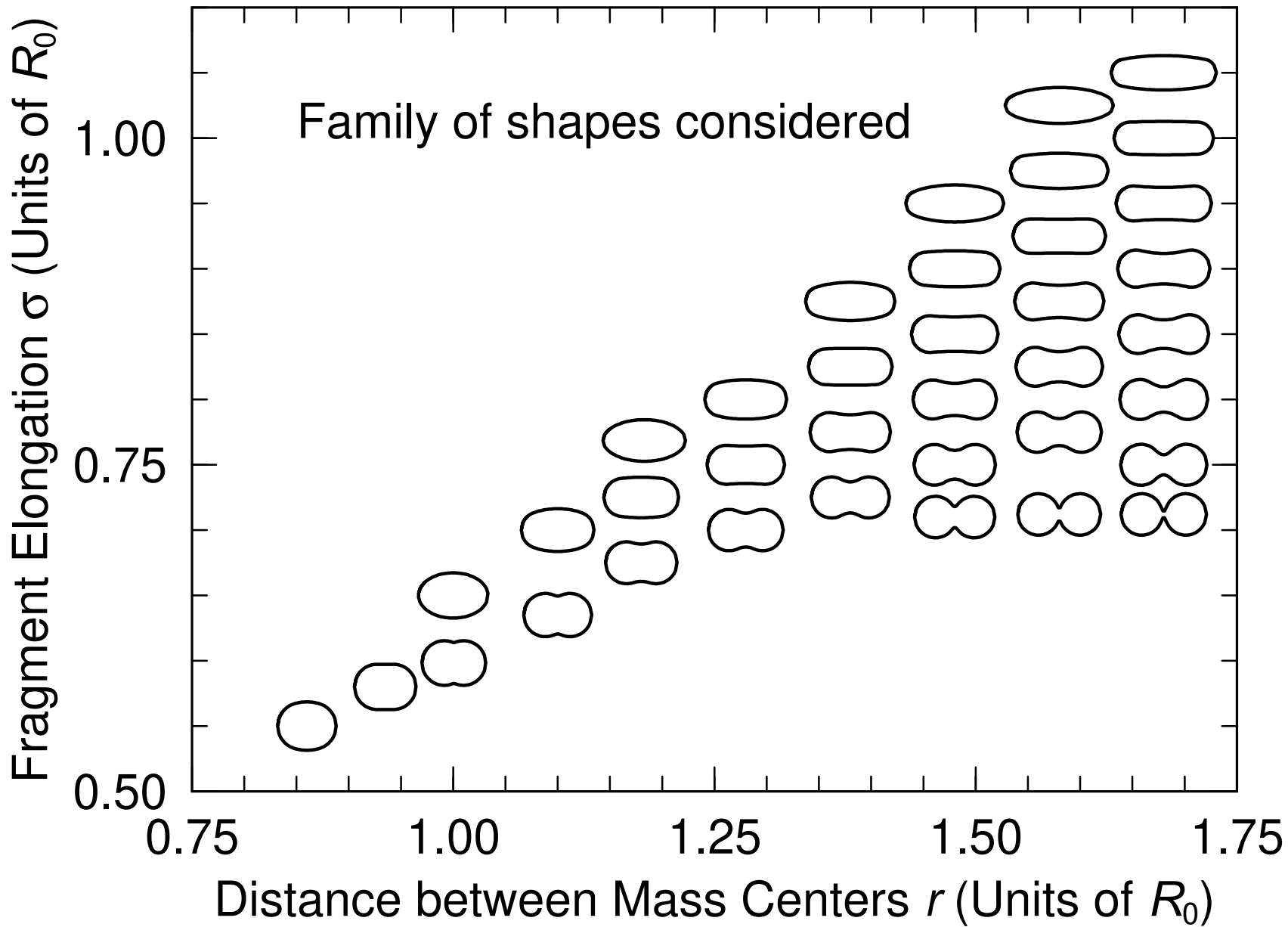
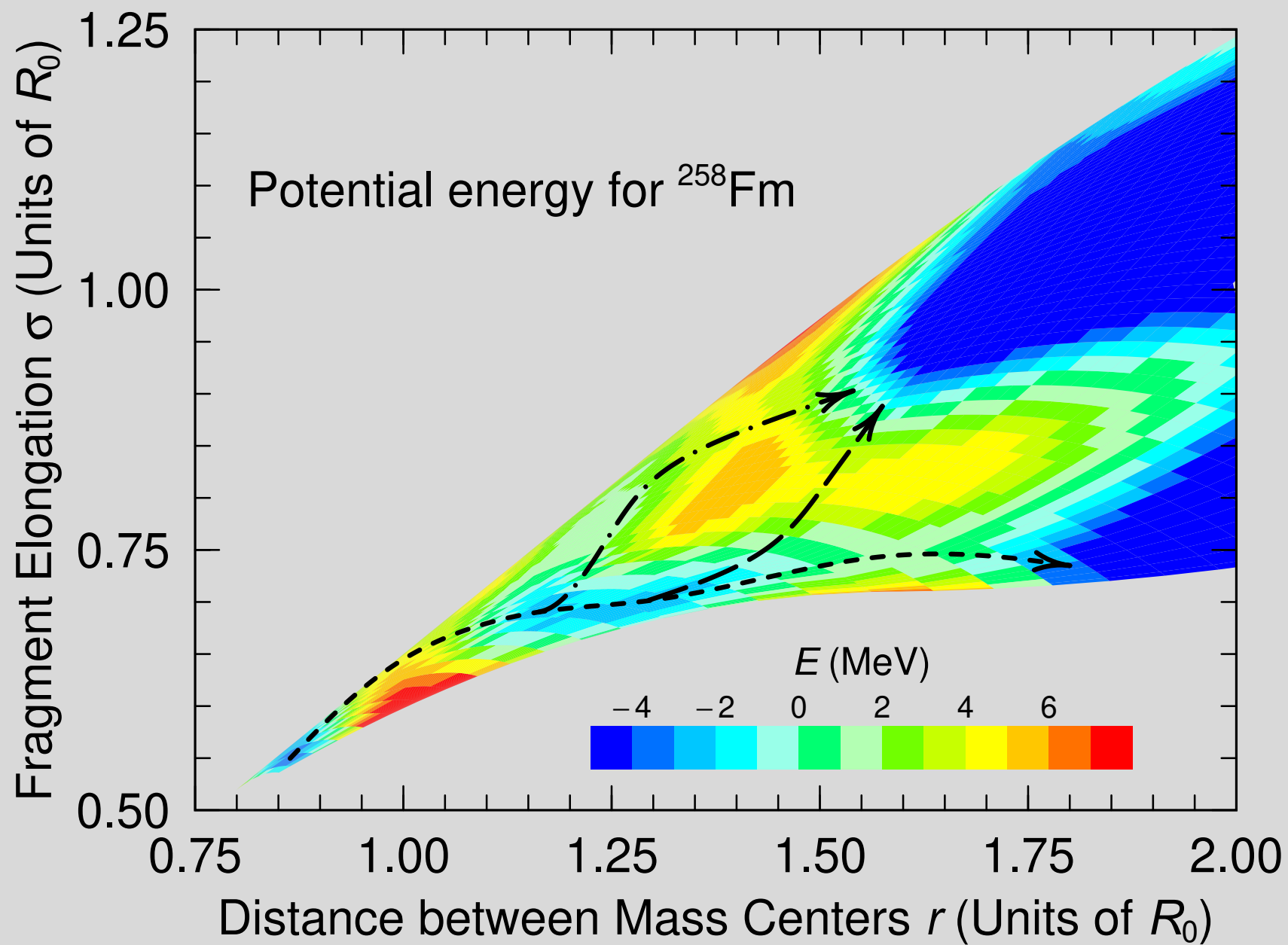
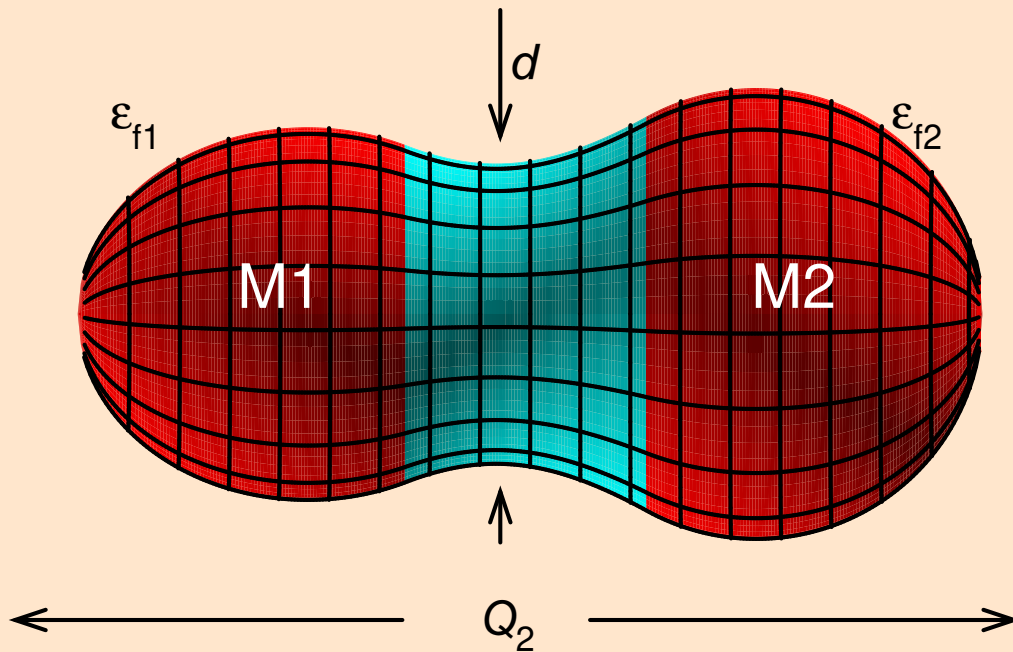


Figure 25





Five Essential Fission Shape Coordinates

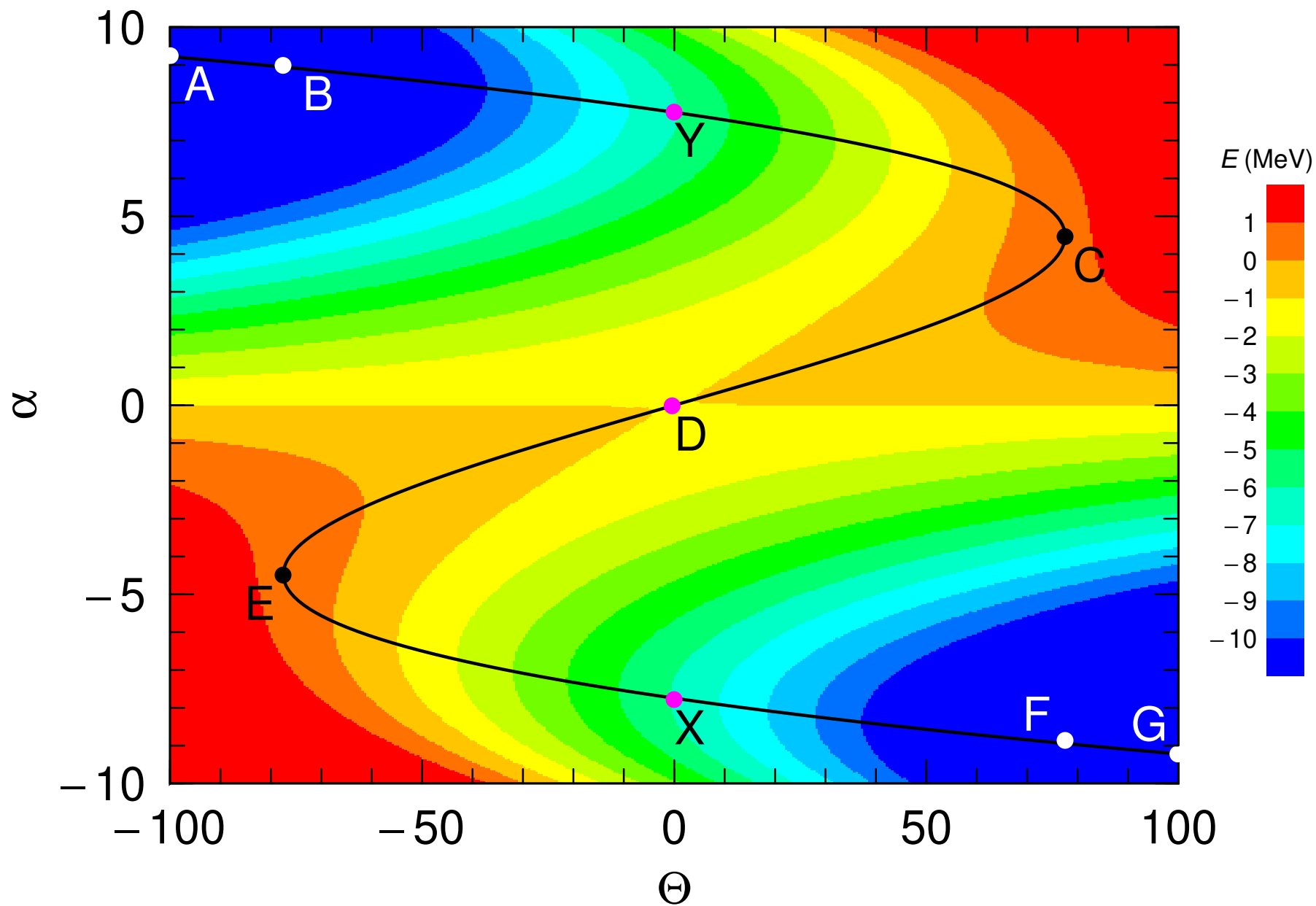


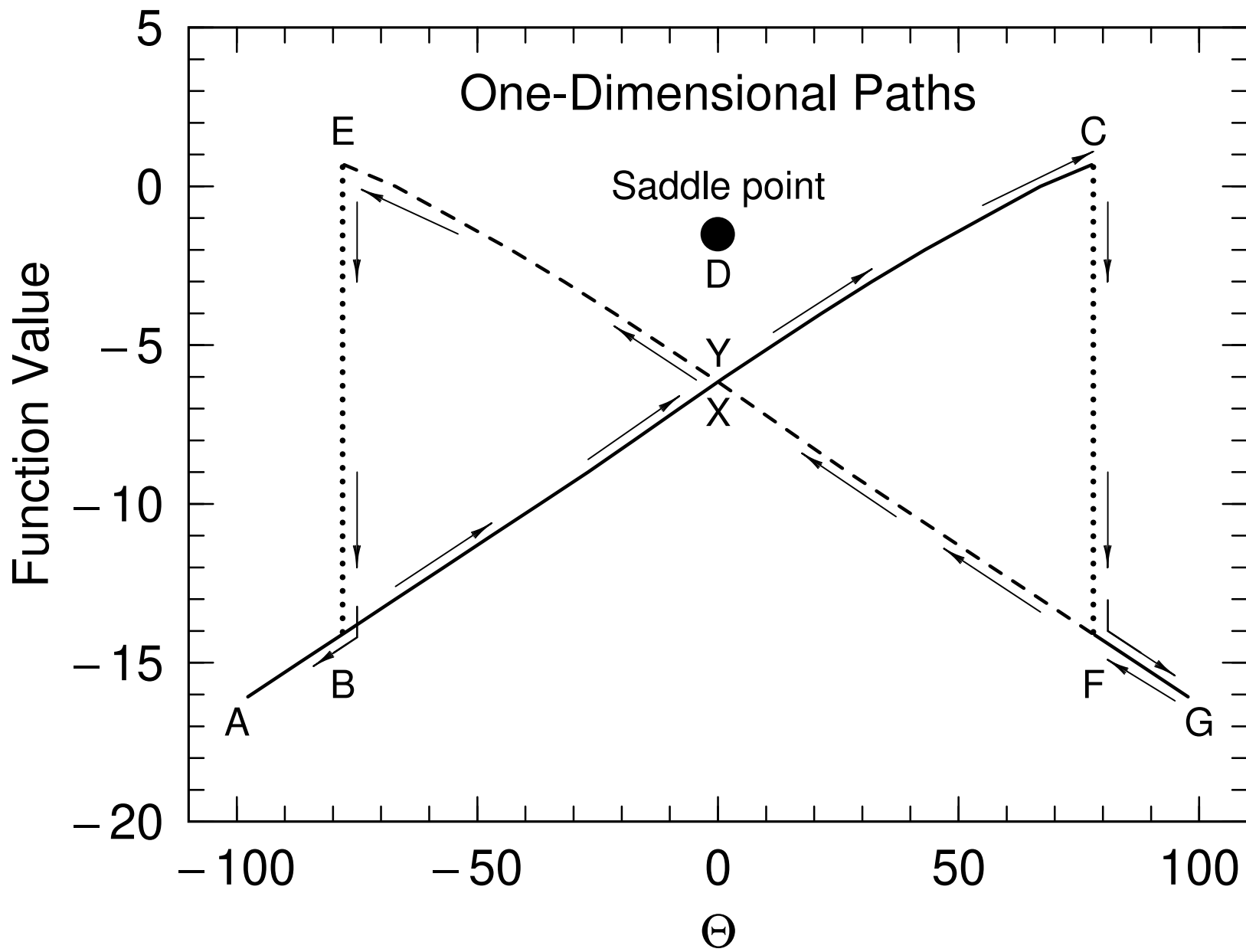
45	$Q_2 \sim$ Elongation (fission direction)
⊗	
35	$\alpha_g \sim (M1-M2)/(M1+M2)$ Mass asymmetry
⊗	
15	$\epsilon_{f1} \sim$ Left fragment deformation
⊗	
15	$\epsilon_{f2} \sim$ Right fragment deformation
⊗	
15	$d \sim$ Neck

⇒ 5 315 625 grid points – 306 300 unphysical points

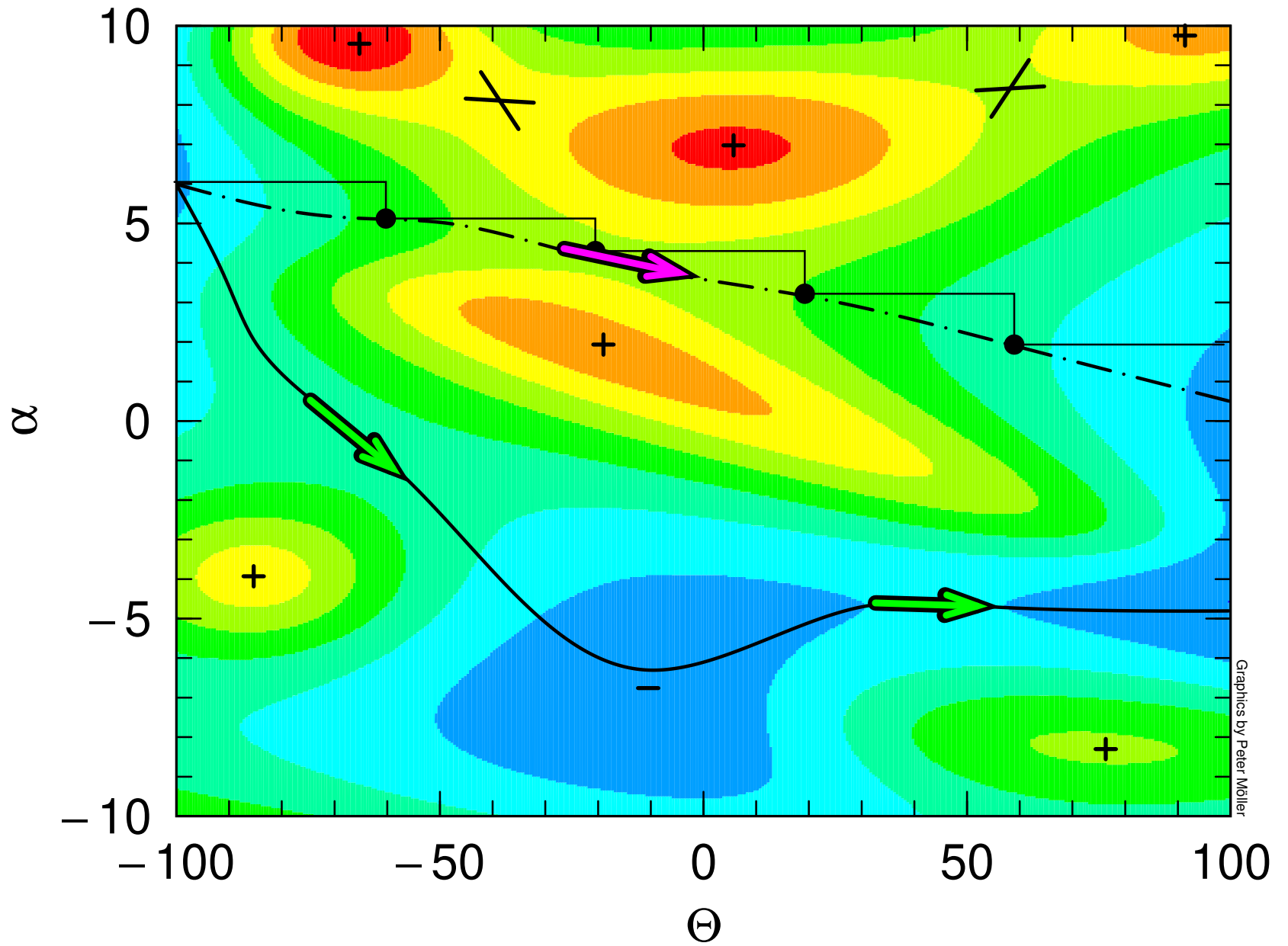
⇒ **5 009 325 physical grid points**

Saddle Search Strategies Illustrated

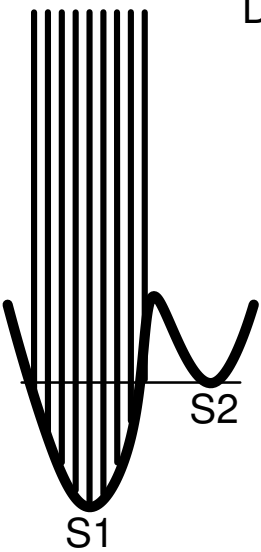




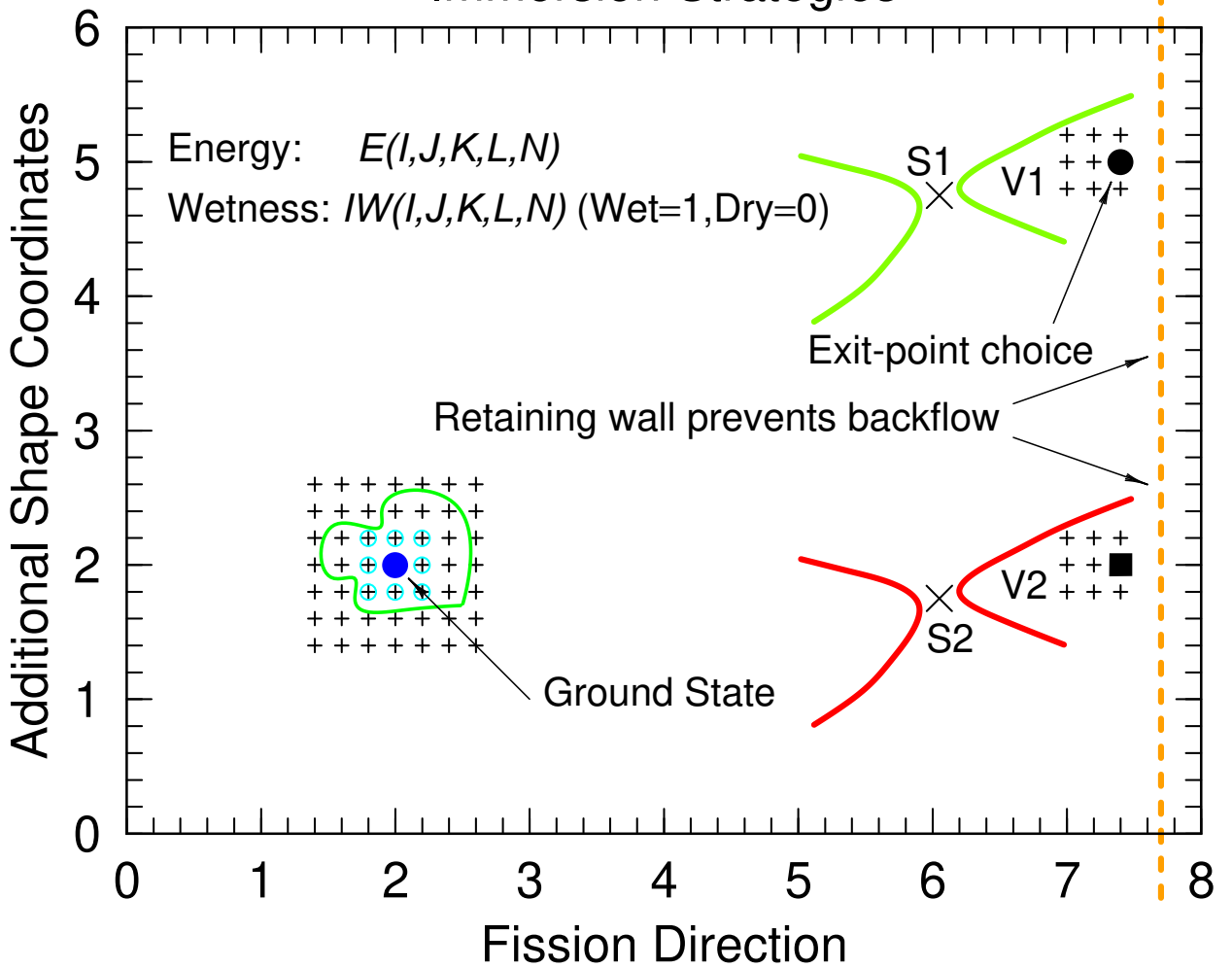
Saddle Search Strategies Illustrated



Dam construction flips water to flow across additional saddle



Immersion Strategies



5D FISSION POTENTIAL ENERGY SURFACE STRUCTURE
 FOR Z = 94 A =240

INTERIOR MINIMA DEEPER THAN 0.20 MeV
 FINAL POINT IS LOWEST POINT AT LARGEST Q2

11	2	11	11	2	0.127
4	1	5	1	30	-2.111
45	1	3	11	8	-41.780

SADDLES BETWEEN ALL PAIRS OF MINIMA ABOVE

11	2	11	11	2	0.127	Entry
8	9	3	3	2	4.021	Saddle
4	1	5	1	30	-2.111	Exit
11	2	11	11	2	0.127	Entry
16	11	10	13	14	2.839	Saddle
45	1	3	11	8	-41.780	Exit
4	1	5	1	30	-2.111	Entry
8	9	3	3	2	4.021	Saddle
45	1	3	11	8	-41.780	Exit

5D FISSION POTENTIAL ENERGY SURFACE VALLEYS FOR Z = 94 A =240

Only Valleys deeper than 2.00 MeV are listed

I	J	K	L	N	E	Q2	MH	ML	EPS-F1	EPS-F2	No	3
32	1	3	1	7	-0.311	99.979	132.0 / 108.0		-0.100	-0.200	1	
32	12	6	7	2	-2.763	99.979	120.0 / 120.0		0.150	0.175	2	
32	6	3	9	9	-5.531	99.979	136.8 / 103.2		-0.100	0.225	3	

Ridges

(1,2)	2.21 (2.52)	Ridge indices-->	32	2	3	1	8
(1,3)	2.21 (2.52)	Ridge indices-->	32	2	3	1	8
(2,3)	-0.42 (2.34)	Ridge indices-->	32	9	5	11	7

I	J	K	L	N	E	Q2	MH	ML	EPS-F1	EPS-F2	No	3
31	1	2	7	34	8.980	92.998	196.8 / 43.2		-0.150	0.175	1	
31	13	11	9	3	-2.210	92.998	122.4 / 117.6		0.275	0.225	2	
31	7	3	12	8	-4.636	92.998	134.4 / 105.6		-0.100	0.300	3	

Ridges

(1,2)	13.66 (4.68)	Ridge indices-->	31	1	7	5	27
(1,3)	13.66 (4.68)	Ridge indices-->	31	1	7	5	27
(2,3)	0.87 (3.08)	Ridge indices-->	31	10	6	11	7

I	J	K	L	N	E	Q2	MH	ML	EPS-F1	EPS-F2	No	3
30	1	2	2	34	9.089	86.121	196.8 / 43.2		-0.150	-0.150	1	
30	13	11	10	3	-2.149	86.121	122.4 / 117.6		0.275	0.250	2	
30	7	3	11	8	-3.642	86.121	134.4 / 105.6		-0.100	0.275	3	

Ridges

(1,2)	17.71 (8.62)	Ridge indices-->	30	2	7	7	28
(1,3)	17.71 (8.62)	Ridge indices-->	30	2	7	7	28
(2,3)	1.97 (4.12)	Ridge indices-->	30	11	6	11	6

I	J	K	L	N	E	Q2	MH	ML	EPS-F1	EPS-F2	No	2
29	13	5	5	2	-1.708	79.358	120.0 / 120.0		0.100	0.100	1	
29	8	3	12	8	-2.613	79.358	134.4 / 105.6		-0.100	0.300	2	

Ridges

(1,2)	3.08 (4.78)	Ridge indices-->	29	11	7	9	8
-------	--------	-------	------------------	----	----	---	---	---

I	J	K	L	N	E	Q2	MH	ML	EPS-F1	EPS-F2	No	2
28	13	5	4	5	-1.465	76.044	127.2 / 112.8		0.100	0.000	1	
28	8	3	11	8	-2.011	76.044	134.4 / 105.6		-0.100	0.275	2	

Ridges

(1,2)	3.29 (4.76)	Ridge indices-->	28	11	6	12	6
-------	--------	-------	------------------	----	----	---	----	---

I	J	K	L	N	E	Q2	MH	ML	EPS-F1	EPS-F2	No	2
27	13	4	4	2	-1.108	72.729	120.0 / 120.0		0.000	0.000	1	
27	8	4	12	9	-1.232	72.729	136.8 / 103.2		0.000	0.300	2	

Ridges

(1,2) 3.15 (4.26) Ridge indices--> 27 11 4 10 10

I	J	K	L	N	E	Q2	MH	ML	EPS-F1	EPS-F2	No	2
26	13	5	5	2	-0.326	69.490	120.0 / 120.0		0.100	0.100	1	
26	8	4	12	9	-0.574	69.490	136.8 / 103.2		0.000	0.300	2	

Ridges

(1,2) 3.11 (3.44) Ridge indices--> 26 11 6 12 7

I	J	K	L	N	E	Q2	MH	ML	EPS-F1	EPS-F2	No	2
25	13	5	6	2	0.868	66.251	120.0 / 120.0		0.100	0.150	1	
25	9	3	9	9	-0.040	66.251	136.8 / 103.2		-0.100	0.225	2	

Ridges

(1,2) 3.03 (2.16) Ridge indices--> 25 11 4 8 11

I	J	K	L	N	E	Q2	MH	ML	EPS-F1	EPS-F2	No	1
24	9	4	9	11	0.493	63.129	141.6 / 98.4		0.000	0.225	1	

I	J	K	L	N	E	Q2	MH	ML	EPS-F1	EPS-F2	No	1
23	9	4	11	10	0.977	60.007	139.2 / 100.8		0.000	0.275	1	

I	J	K	L	N	E	Q2	MH	ML	EPS-F1	EPS-F2	No	1
22	9	4	13	8	1.216	57.176	134.4 / 105.6		0.000	0.350	1	

I	J	K	L	N	E	Q2	MH	ML	EPS-F1	EPS-F2	No	1
21	9	4	14	6	1.288	54.346	129.6 / 110.4		0.000	0.400	1	

I	J	K	L	N	E	Q2	MH	ML	EPS-F1	EPS-F2	No	1
20	10	4	10	10	1.467	51.791	139.2 / 100.8		0.000	0.250	1	

I	J	K	L	N	E	Q2	MH	ML	EPS-F1	EPS-F2	No	1
19	10	4	10	10	1.874	49.235	139.2 / 100.8		0.000	0.250	1	

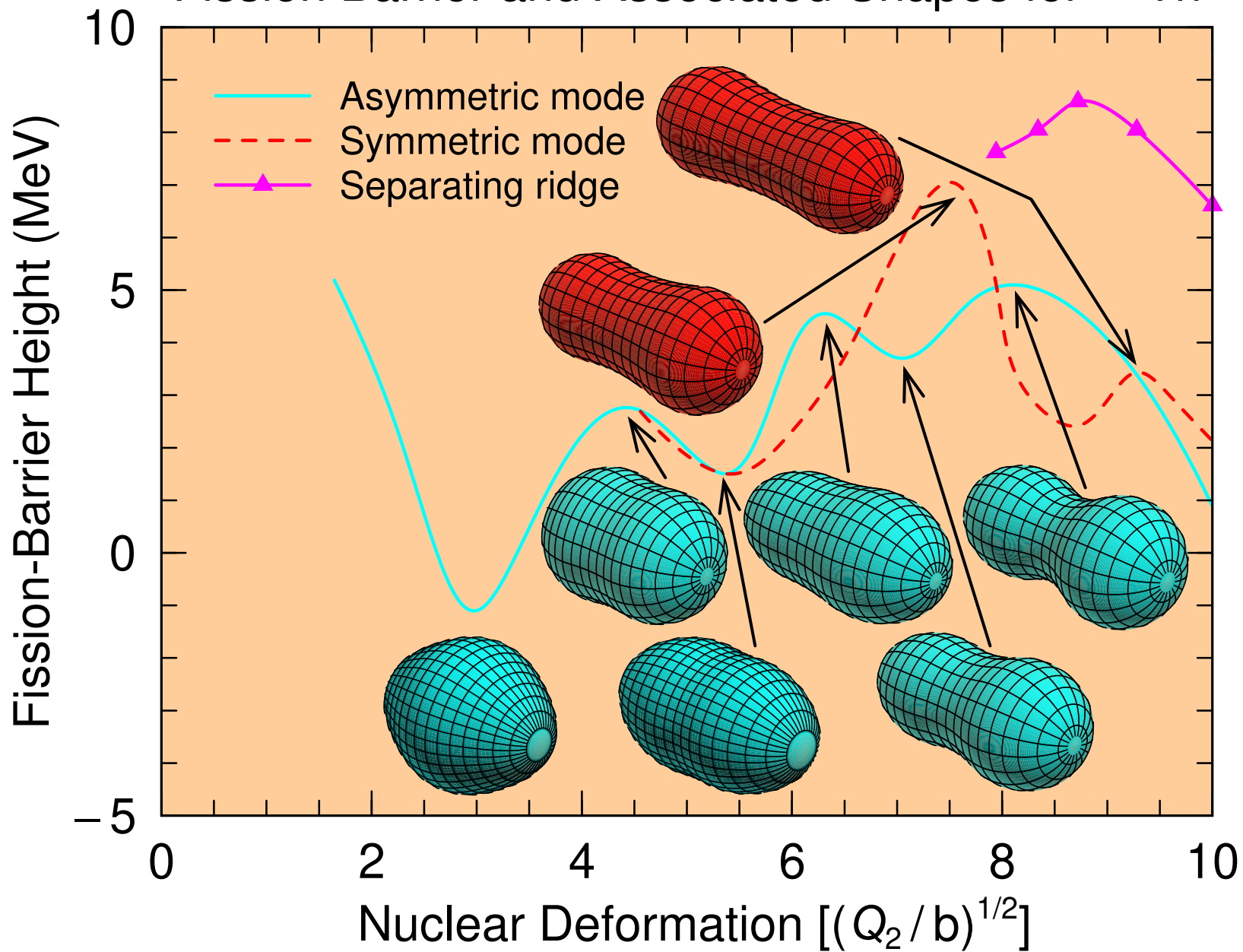
I	J	K	L	N	E	Q2	MH	ML	EPS-F1	EPS-F2	No	1
18	10	5	8	13	2.318	46.914	146.4 / 93.6		0.100	0.200	1	

I	J	K	L	N	E	Q2	MH	ML	EPS-F1	EPS-F2	No	1
17	10	6	9	14	2.744	44.592	148.8 / 91.2		0.150	0.225	1	

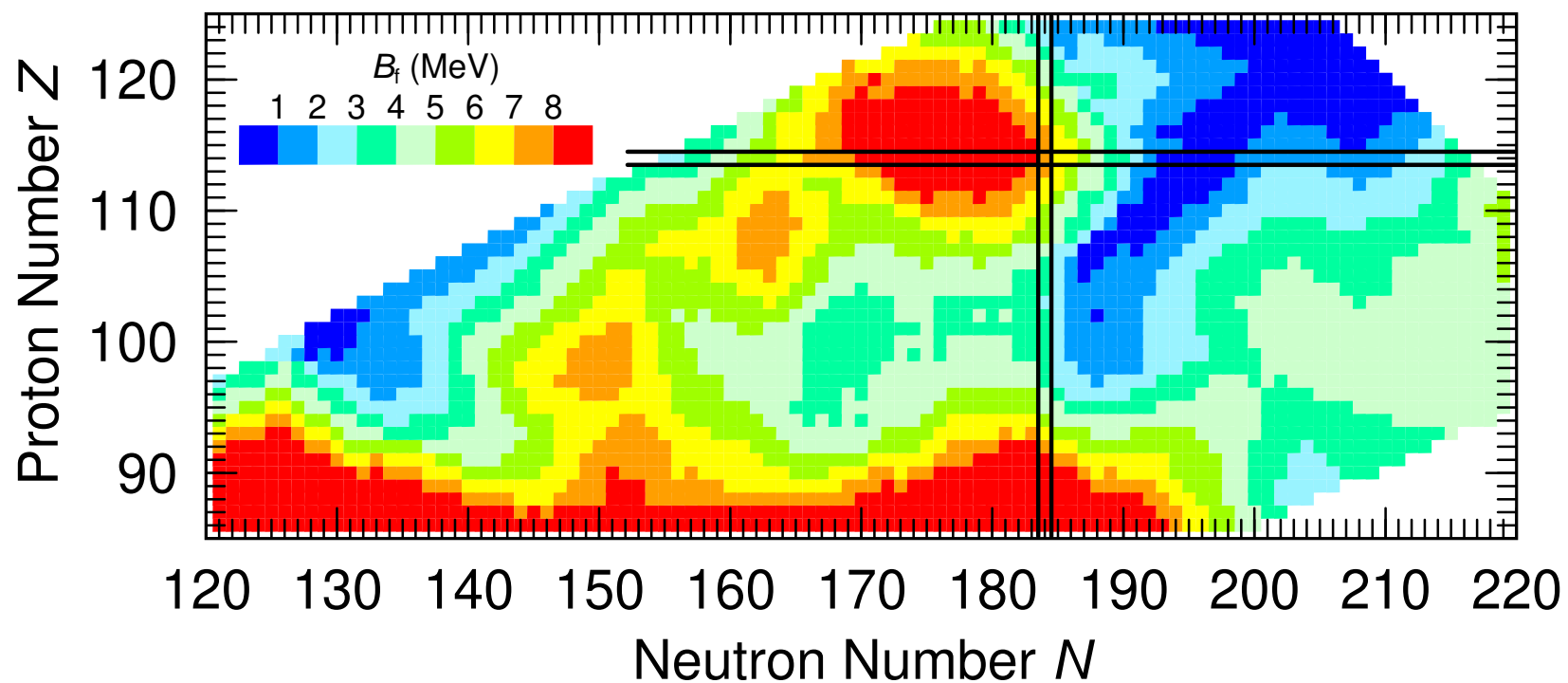
I	J	K	L	N	E	Q2	MH	ML	EPS-F1	EPS-F2	No	1
16	11	12	14	13	2.809	42.471	146.4 / 93.6		0.300	0.400	1	

I	J	K	L	N	E	Q2	MH	ML	EPS-F1	EPS-F2	No	1
15	12	14	15	10	2.718	40.349	139.2 / 100.8		0.400	0.500	1	

Fission Barrier and Associated Shapes for ^{232}Th



Calculated Fission-Barrier Heights



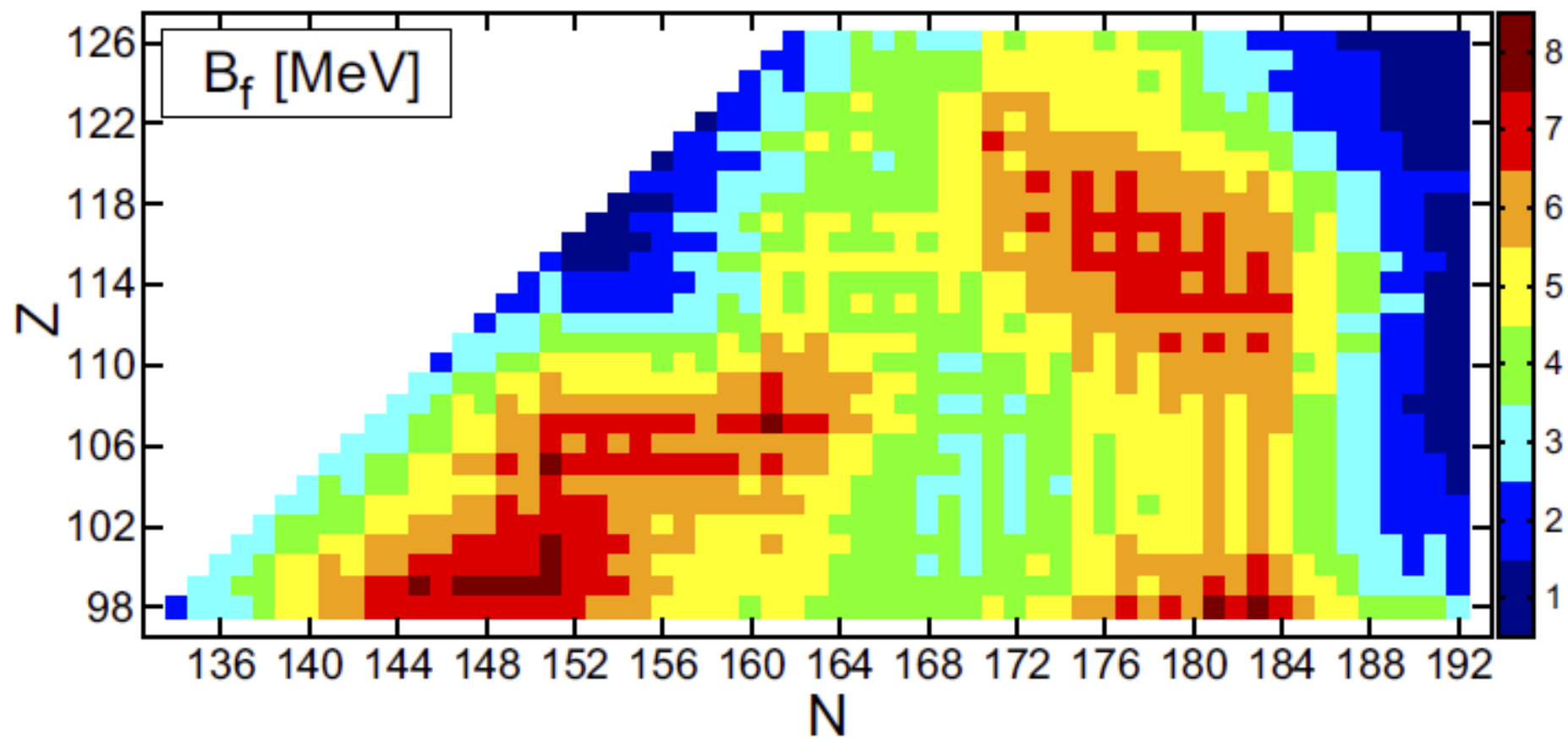
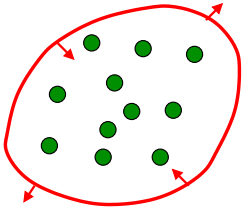


FIG. 19. Calculated fission-barrier heights B_f for superheavy nuclei.



Brownian shape motion

Nuclear deformation energy: $E_{\text{def}}(i,j,k,l,m)$

Bias potential: $V_{\text{bias}}(i) = V_0 (Q_0/Q_2)^2$

Level density parameter: $a_A = A/(8 \text{ MeV})$

Temperature T : $E^* - E_{\text{def}} = a_A T^2$

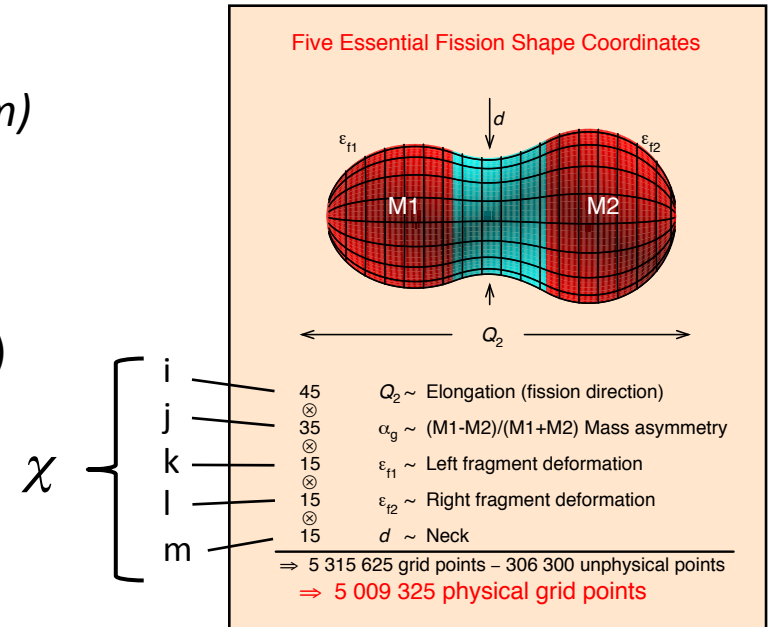
$$\Rightarrow V(\chi) = E_{\text{def}} + V_{\text{bias}}$$

Metropolis walk:

Change shape: $\chi \rightarrow \chi'$?

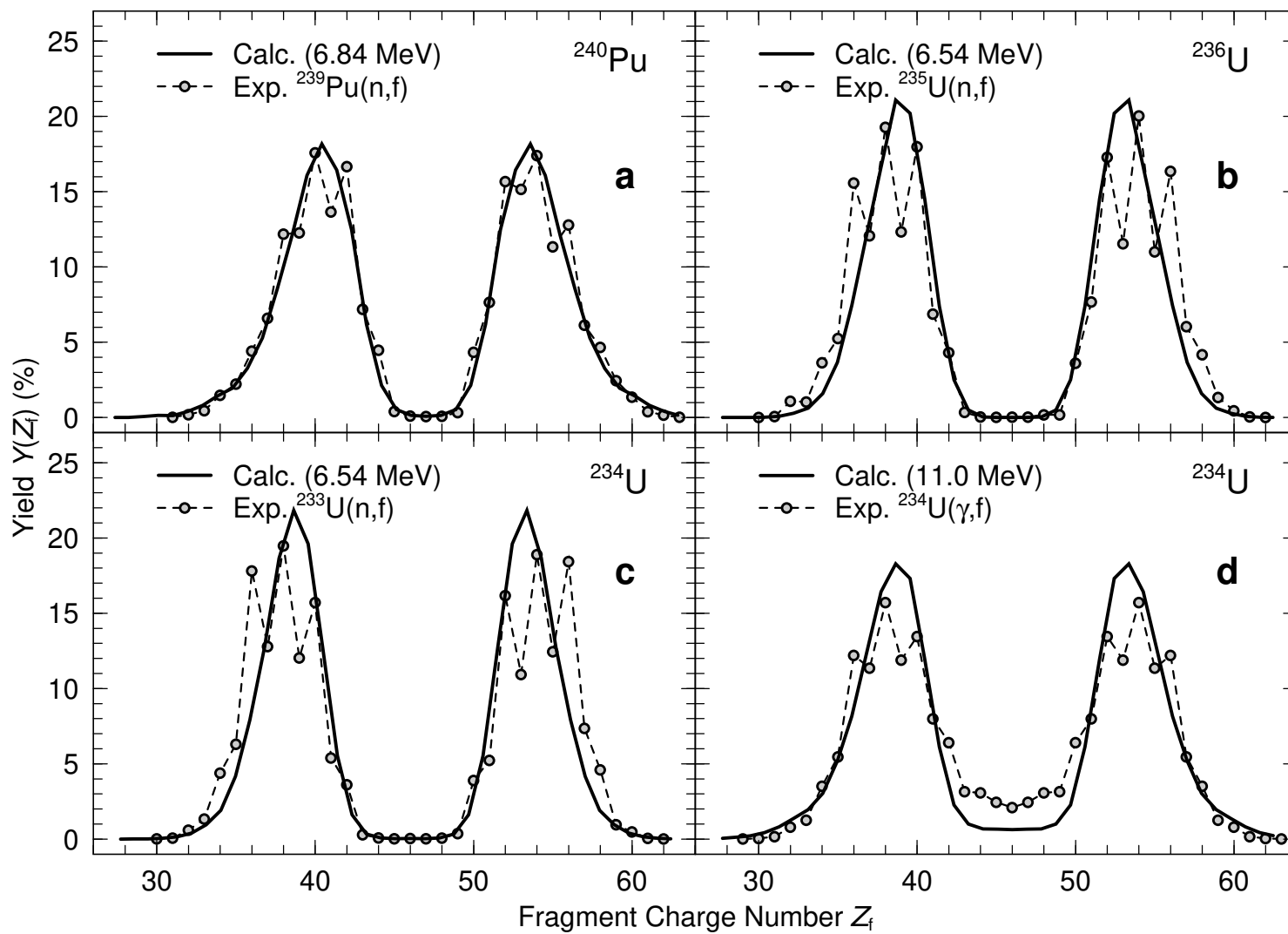
$$\begin{cases} V(\chi') < V(\chi): \text{ move with } P = 1 \\ V(\chi') > V(\chi): \text{ move with } P = \exp(-\Delta V/T) \end{cases}$$

Scission: Critical neck radius $c_0 \approx 2.5 \text{ fm}$

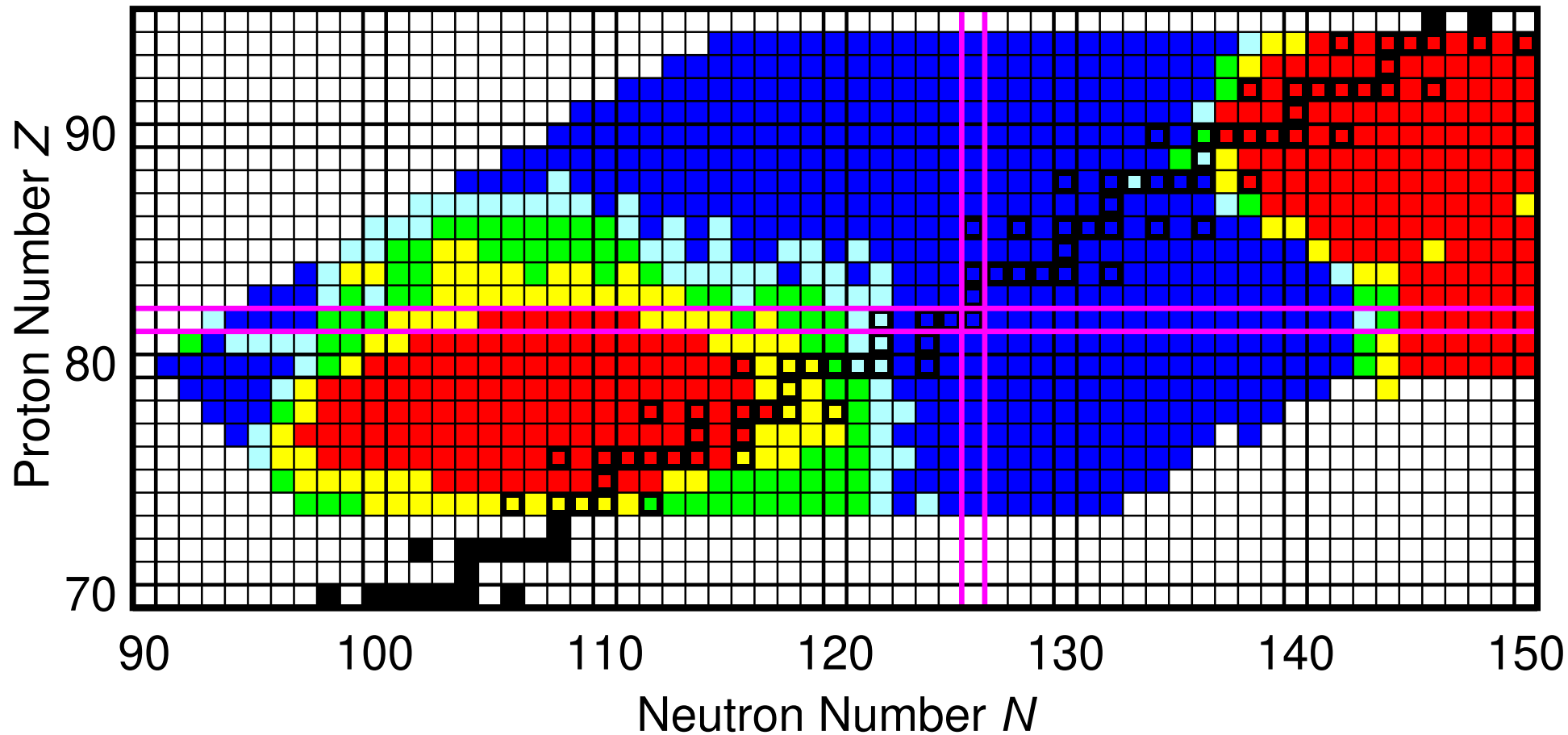


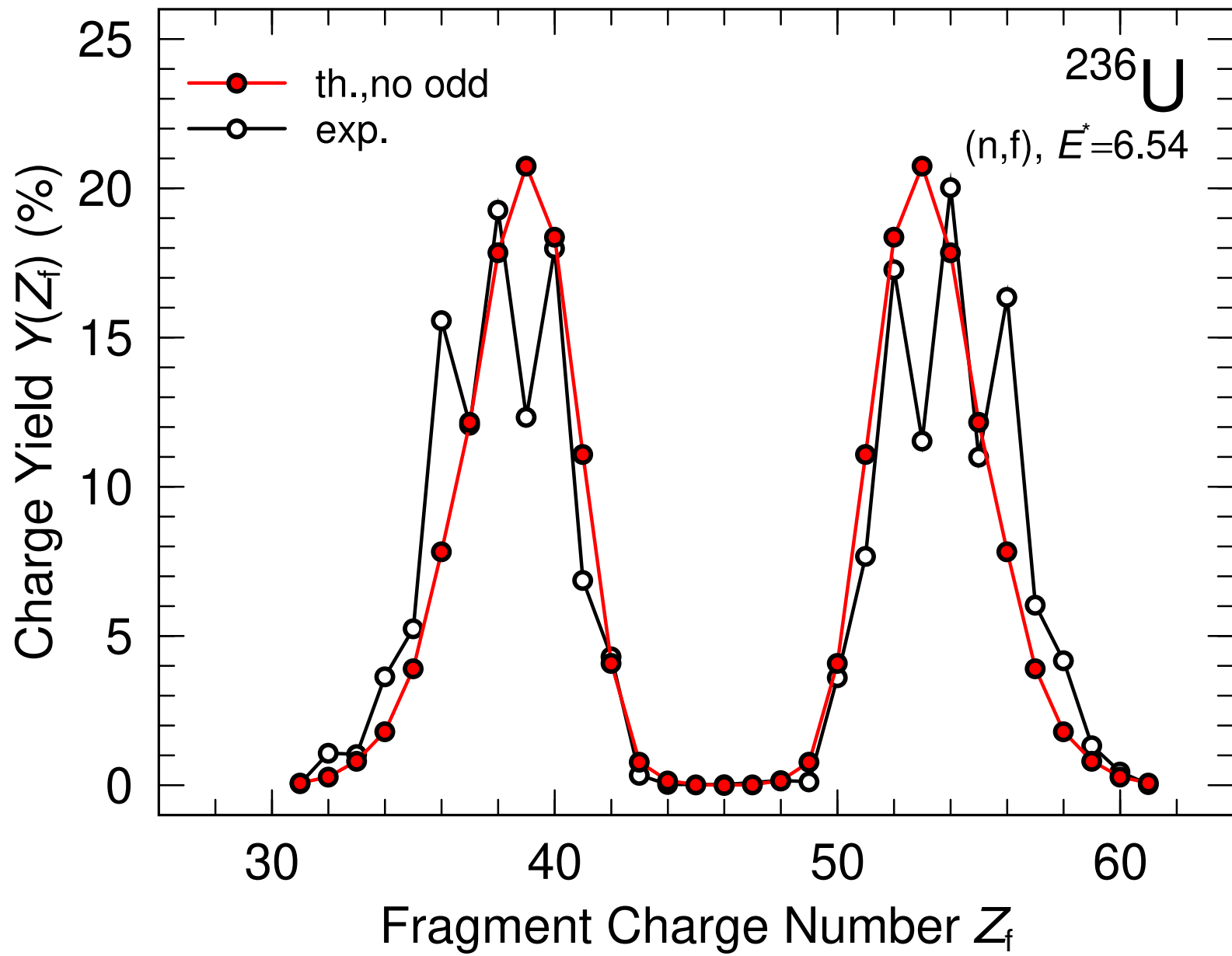
P. Möller *et al*, Nature 409 (2001) 785

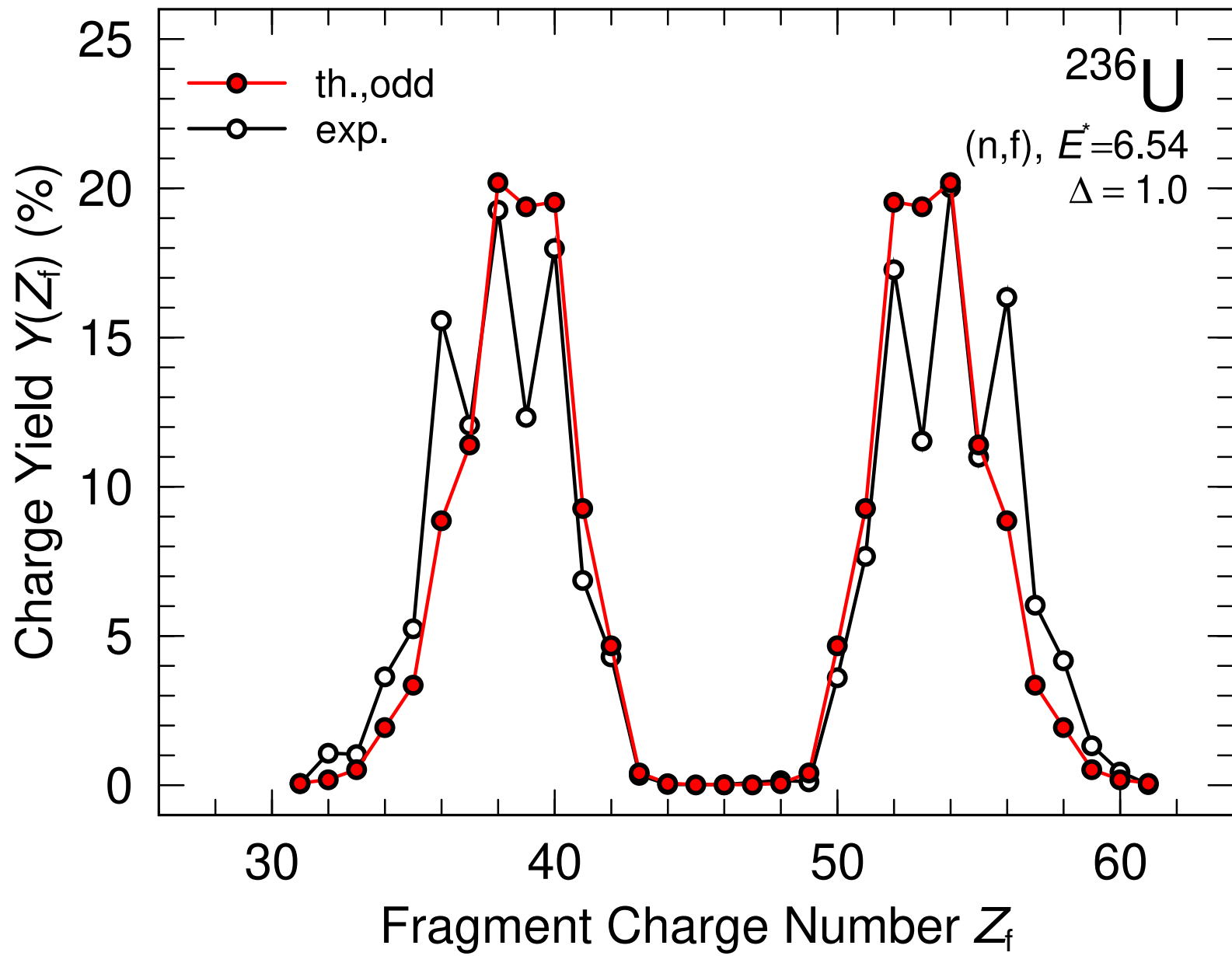
N. Metropolis *et al*, J Chem Phys 26 (1953) 1087



Fission-Fragment Symmetric-Yield to Peak-Yield Ratio







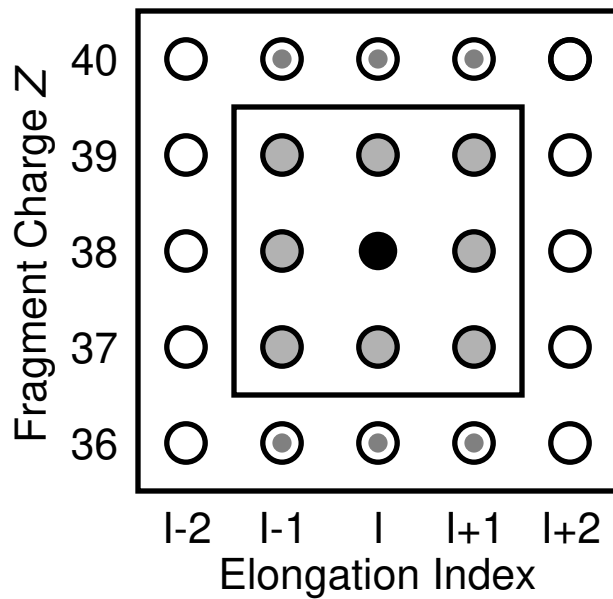


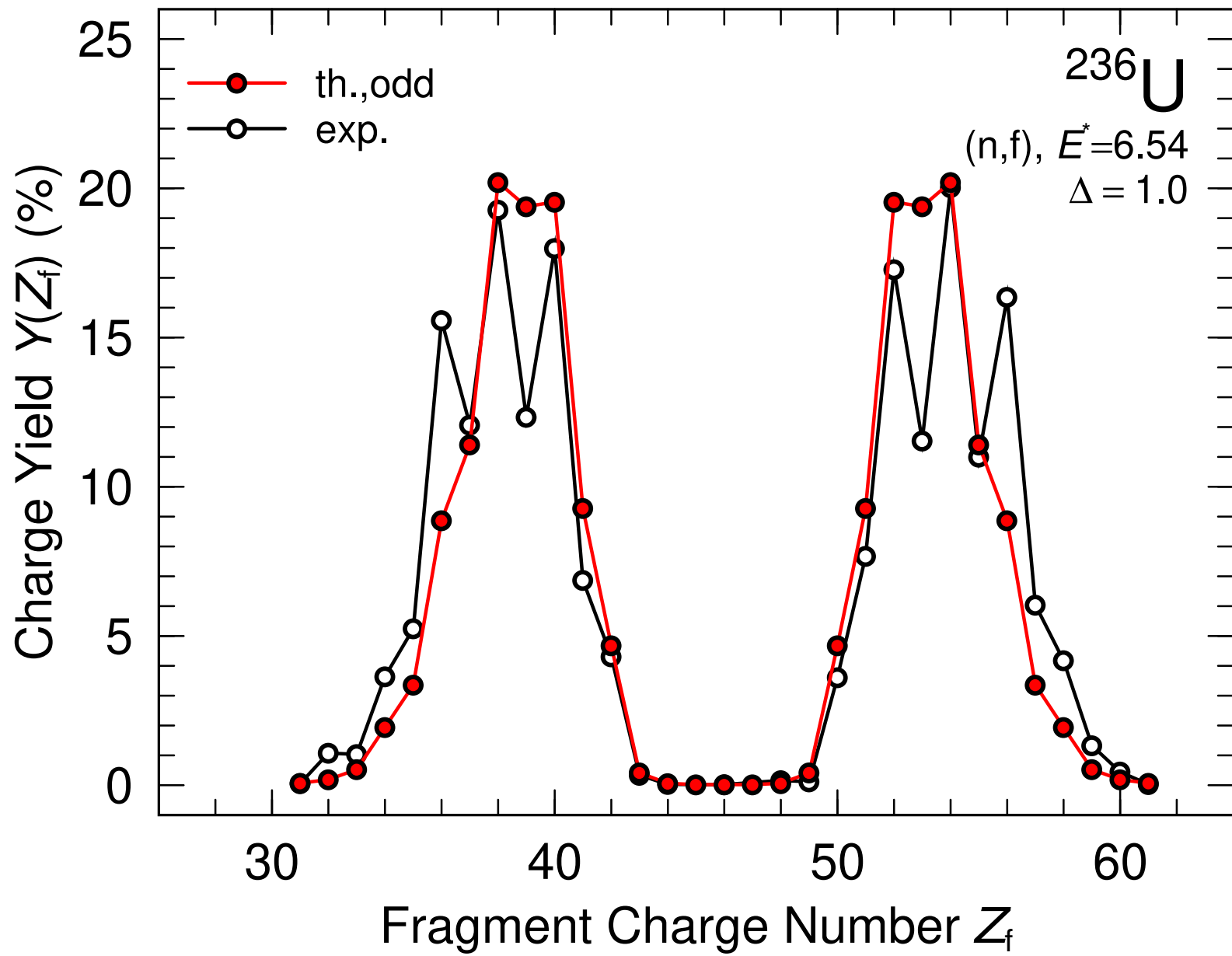


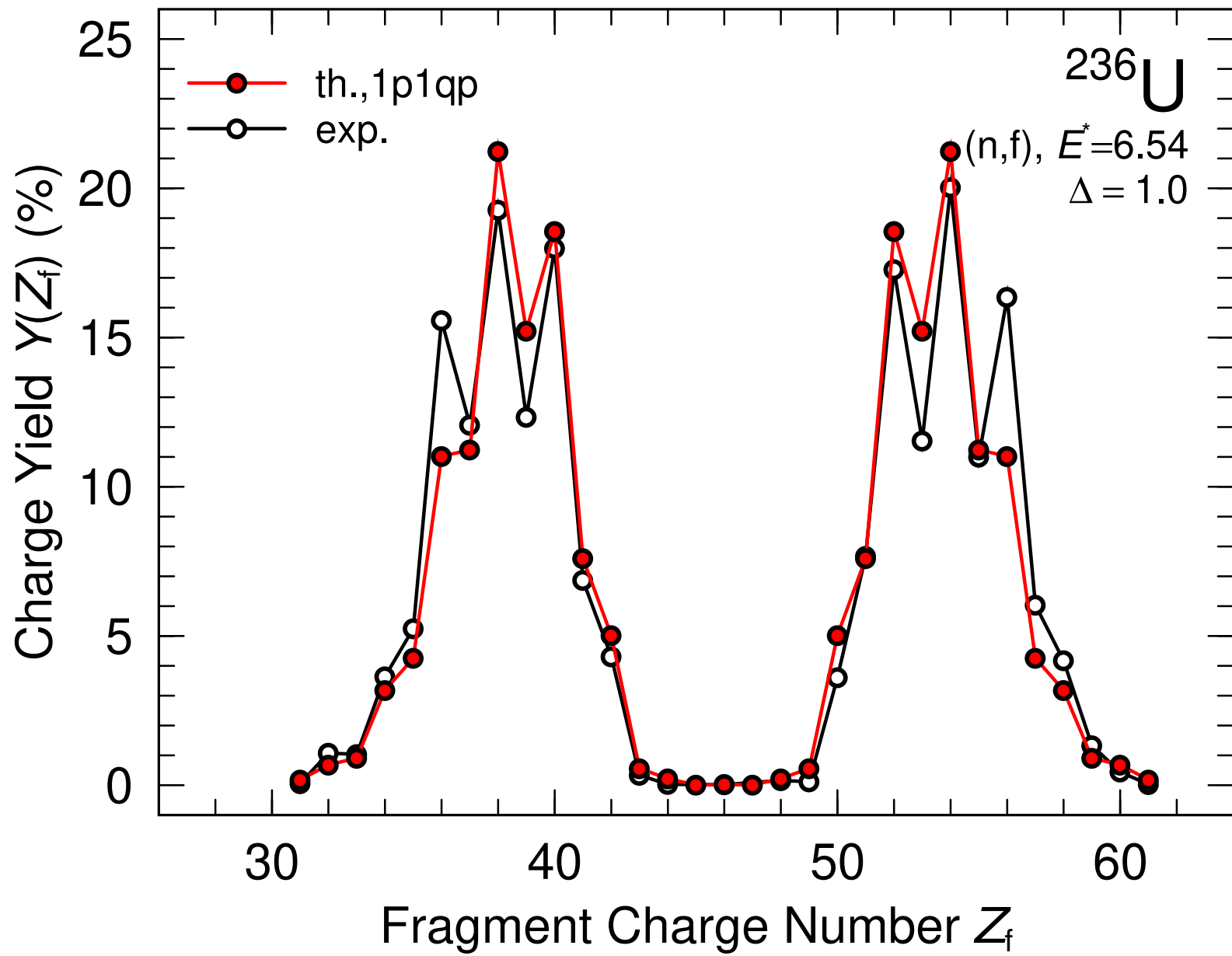


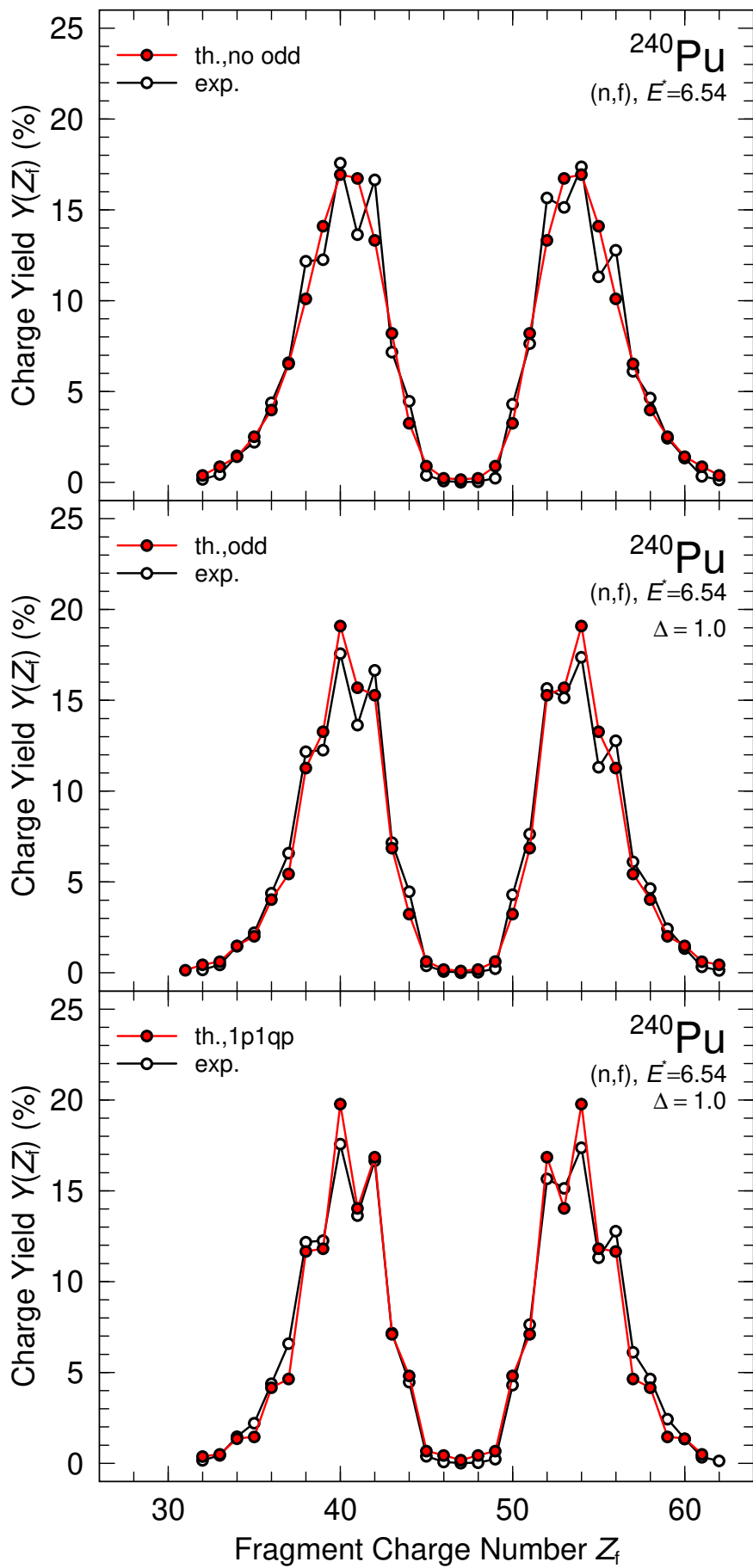


Next Track-Point Candidates



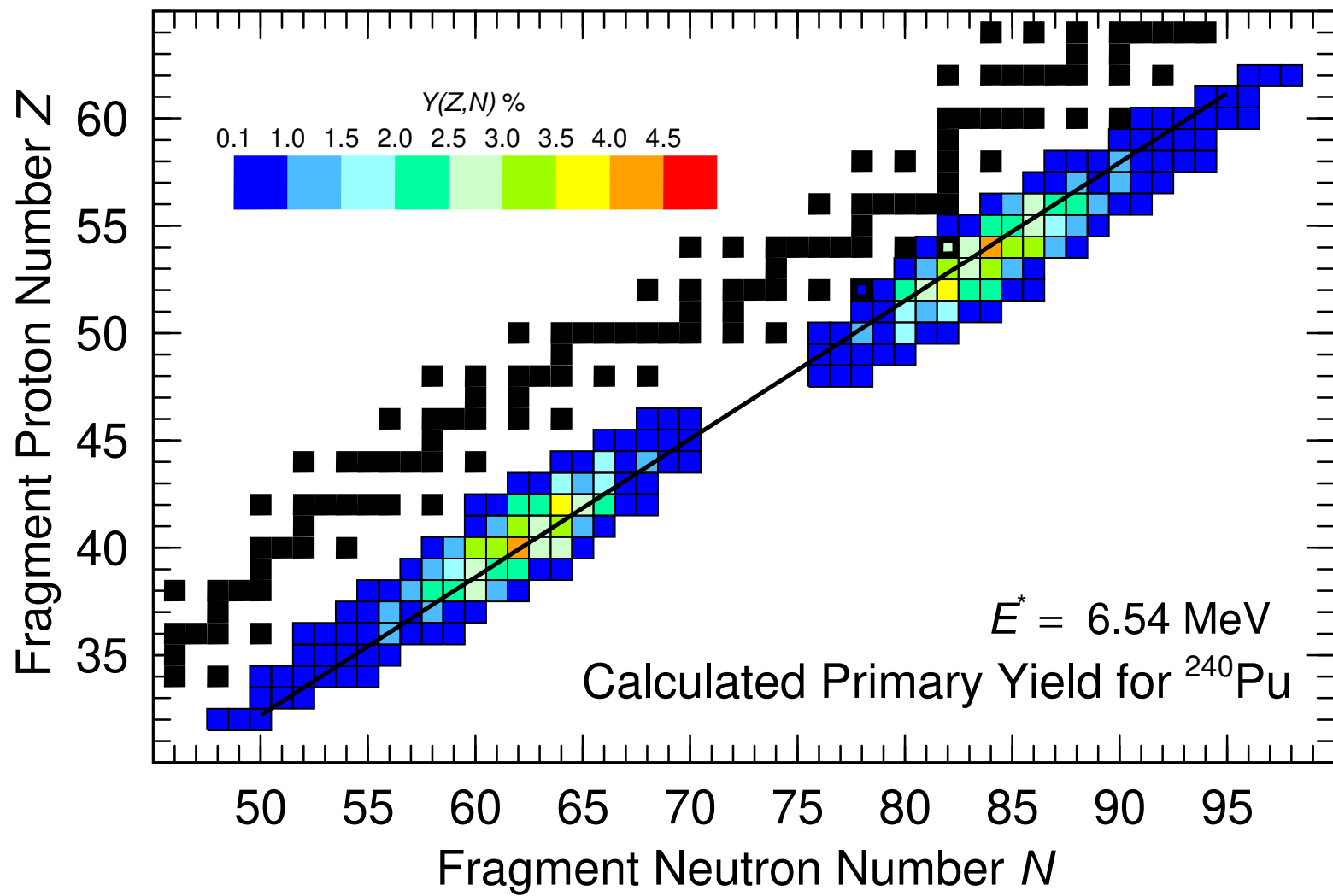


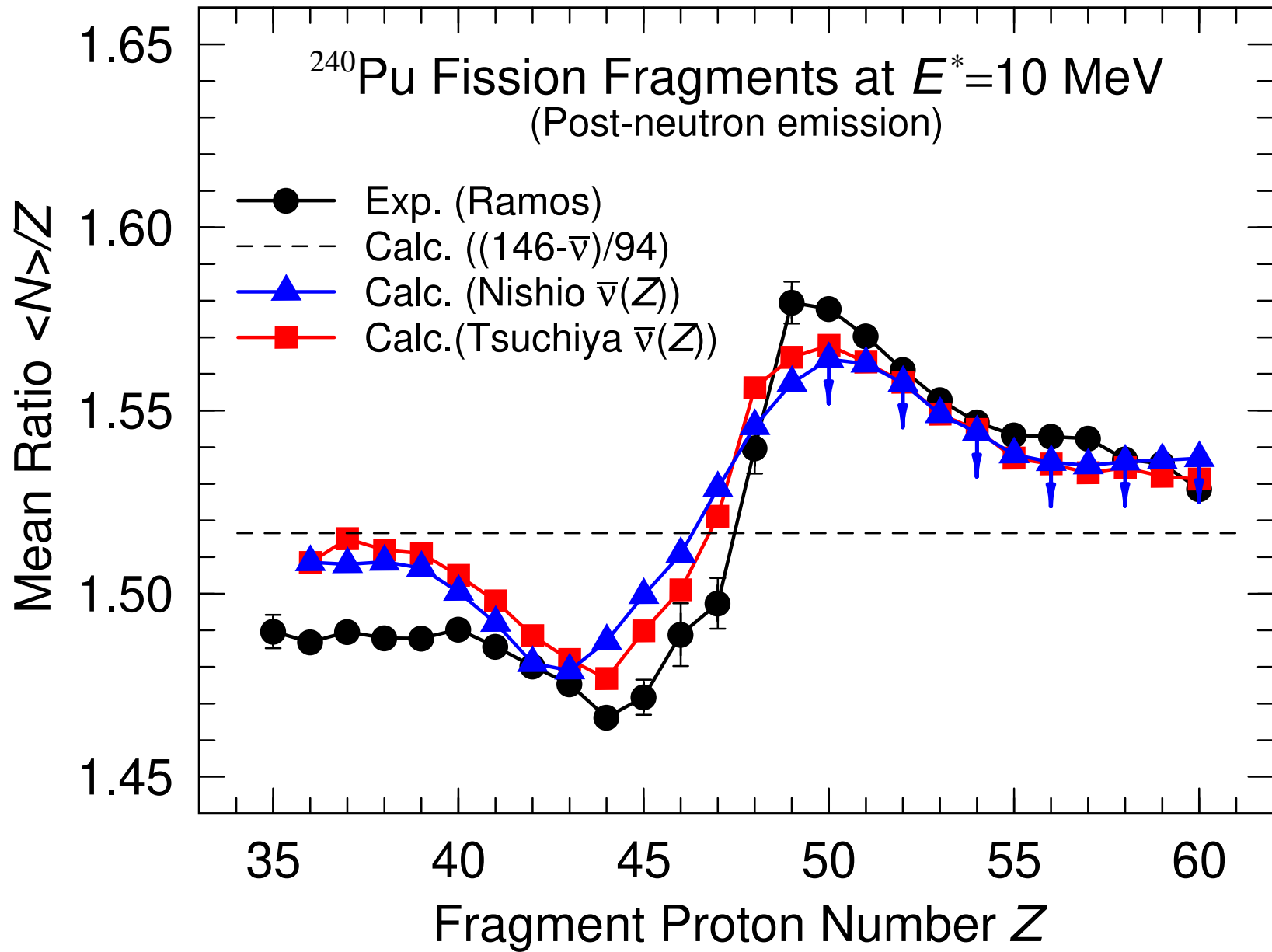


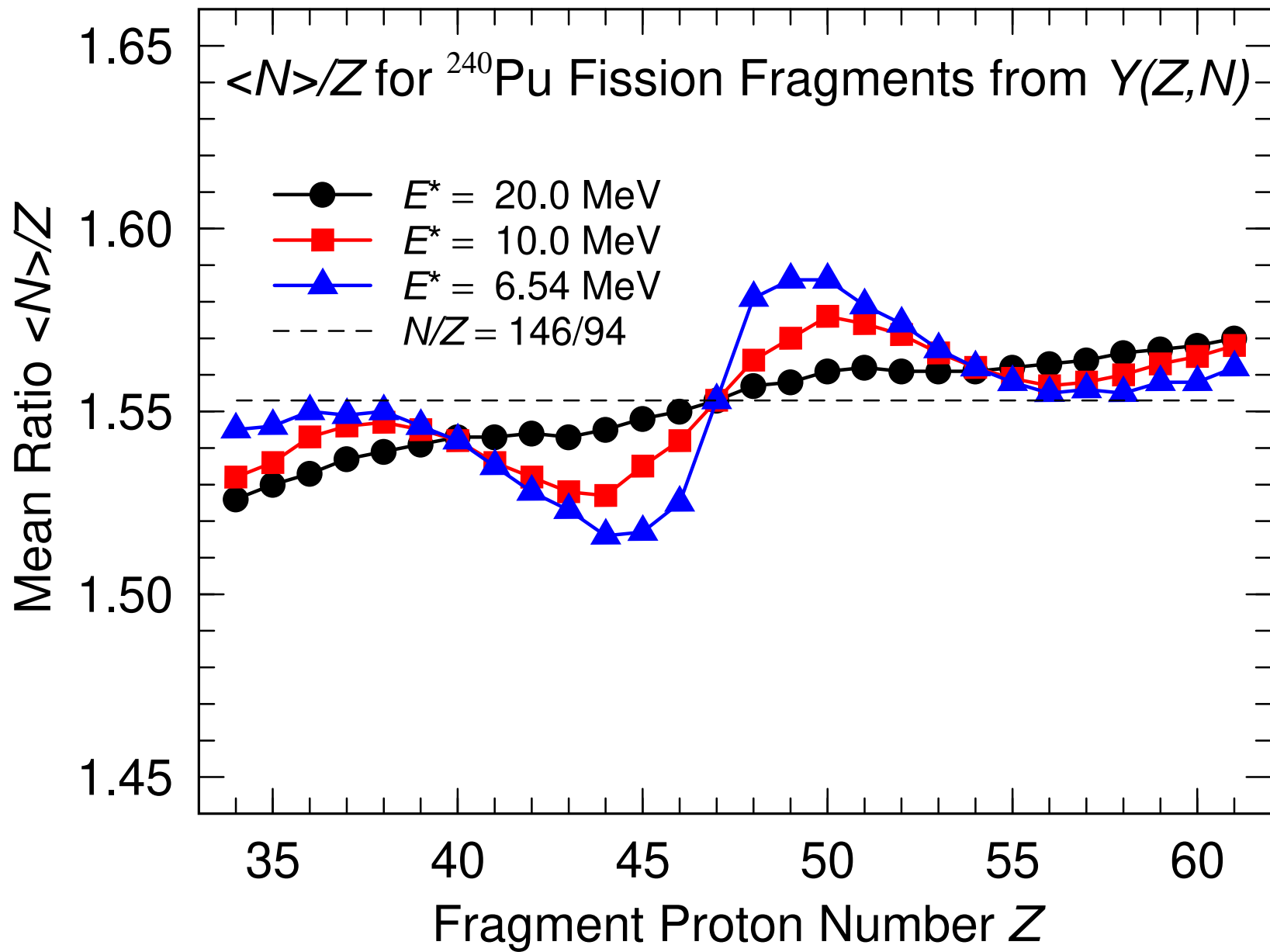


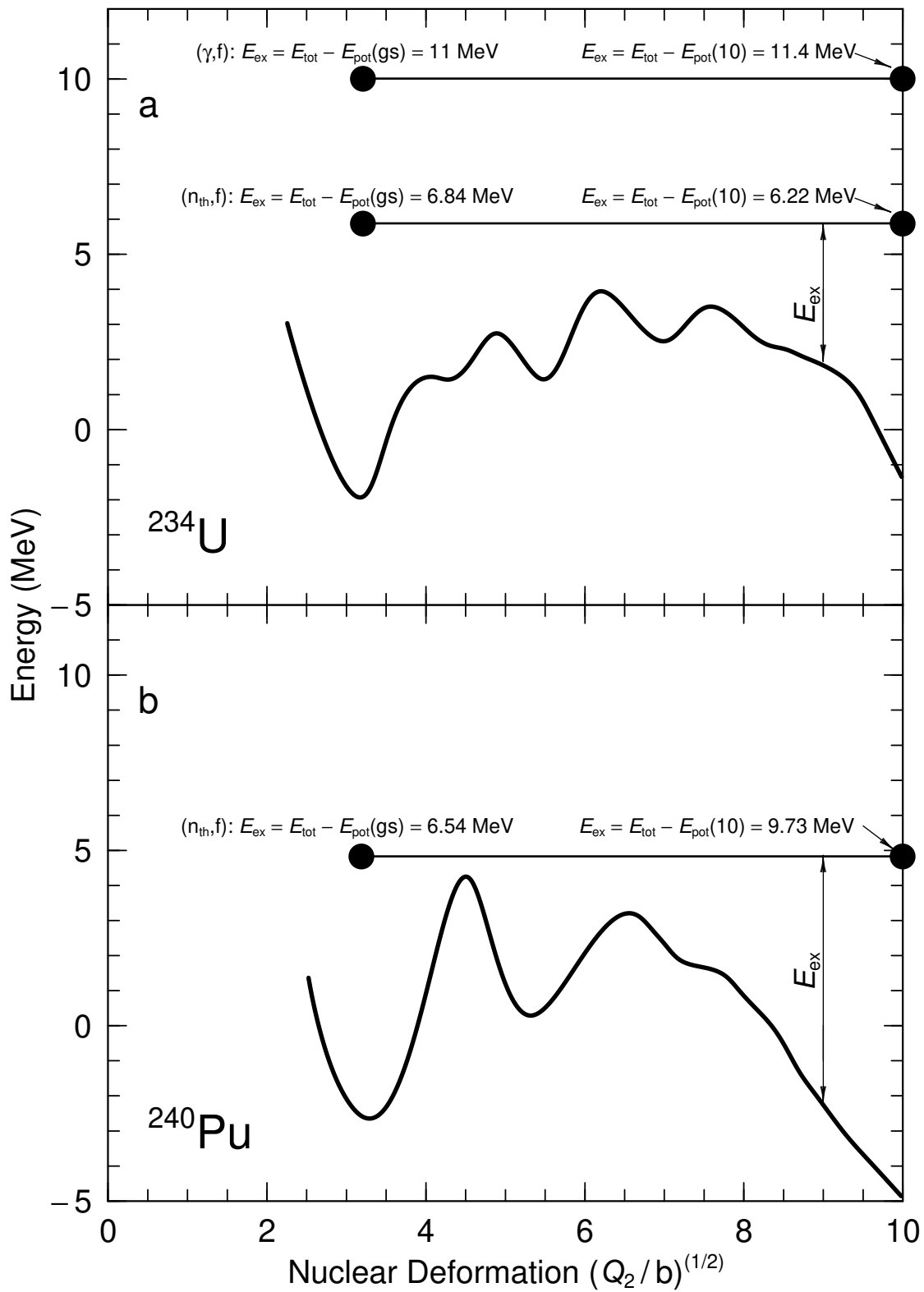
Method for Calculating $E(Q_2, d, \epsilon_{f1}, \epsilon_{f2}, Z_1, N_1)$

- Calculate $E_{SH,n}(N_1)$ for integer N_1 , save
- Calculate $E_{SH,p}(Z_1)$ for integer Z_1 , also save $E_{mac}(Z_1, N(Z_1))$
- Total energy for (Z_x, N_x) split is then $E_{SH,n}(N_x) + E_{SH,p}(Z_x) + E_{mac}(Z_x, N(Z_x)) + \text{Diff}$
- Diff obtained from separated fragment Macroscopic energy difference, see EPJA-051-2015-173.









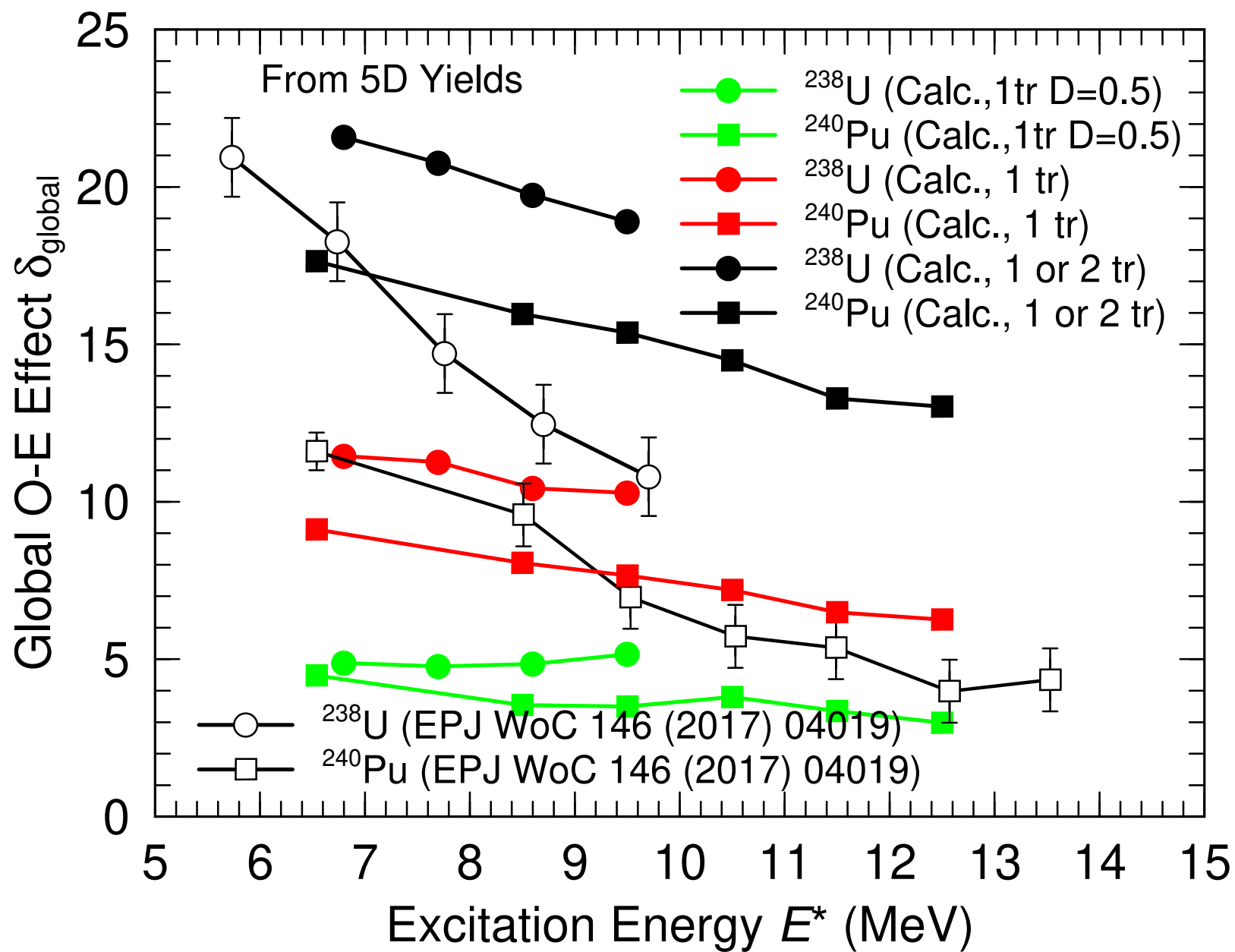
CHARACTERIZATIONS OF STAGGERING

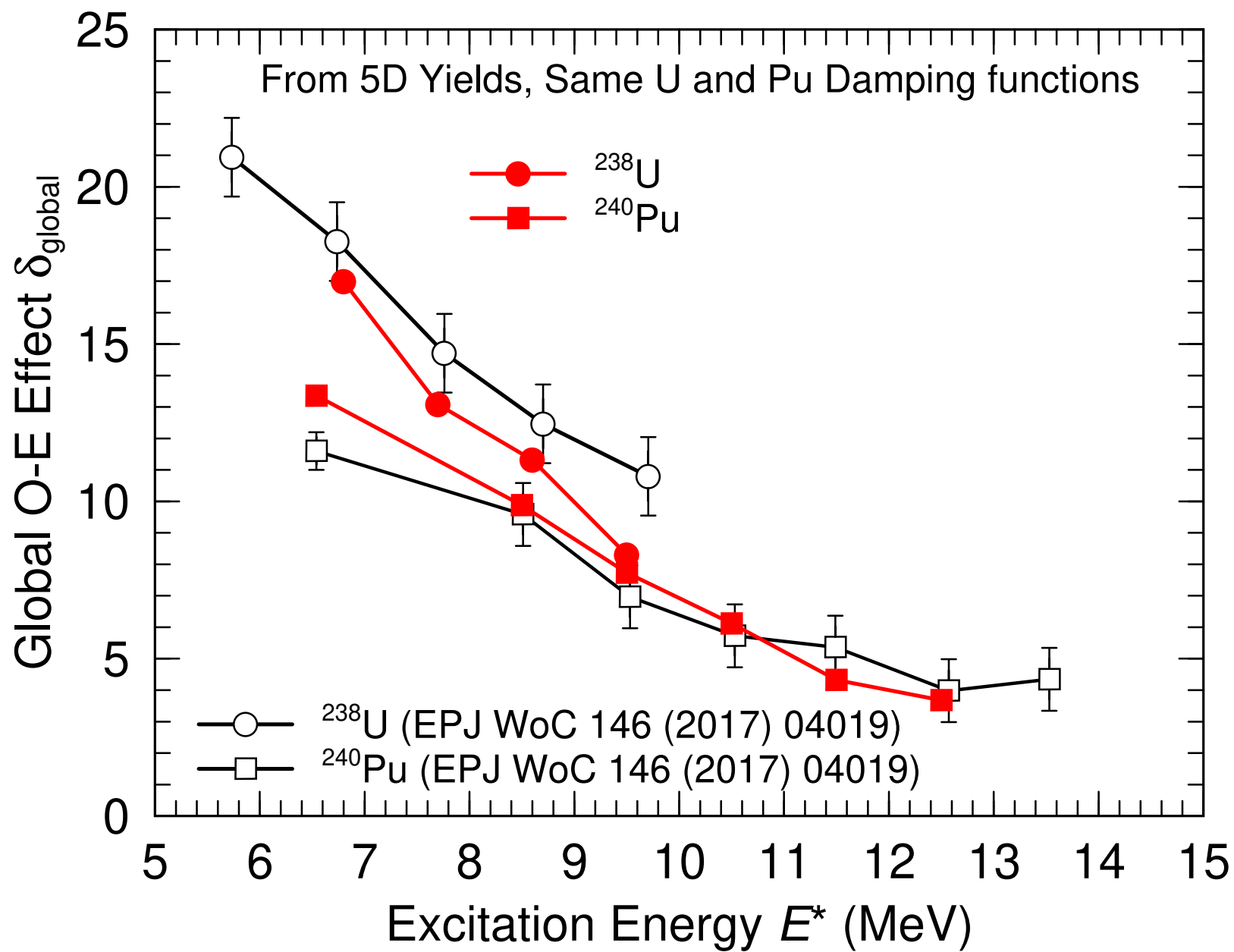
Tracy et al define a local odd-even staggering measure δ_{l-oe} which specifically applied to charge yields is written

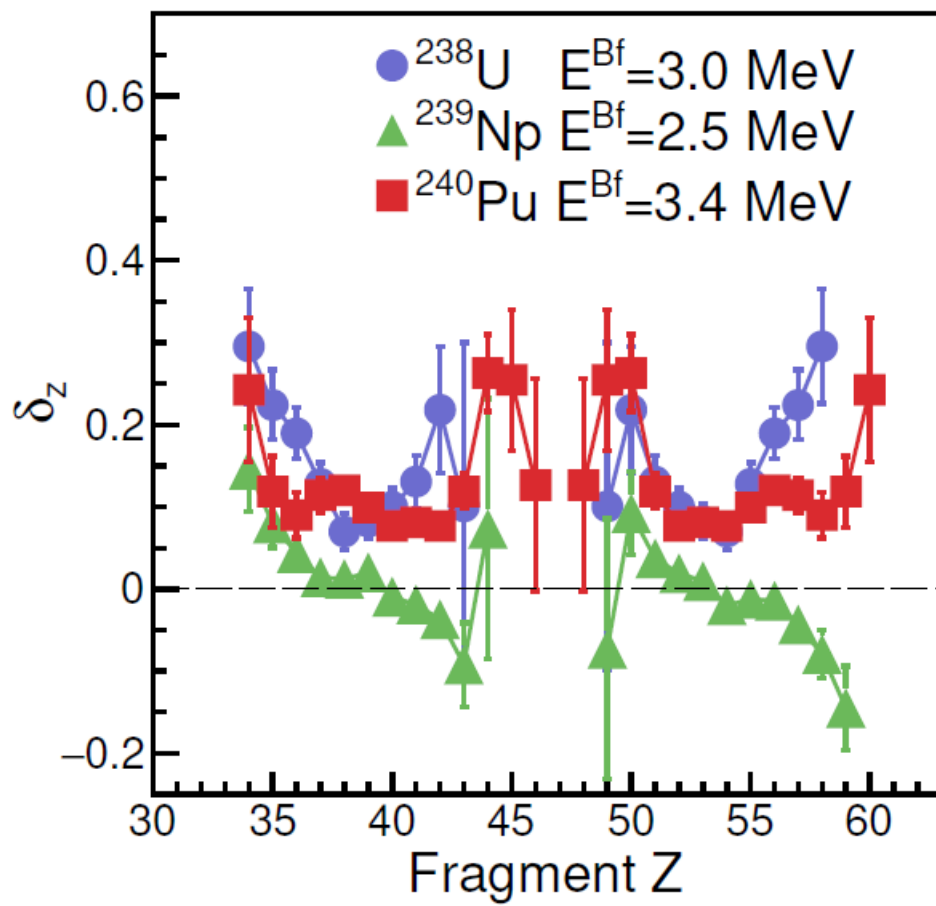
$$\delta_{l-oe} \left(Z + \frac{3}{2} \right) = \frac{(-1)^Z}{8} [\ln Y(Z+3) - \ln Y(Z) - 3(\ln Y(Z+2) - \ln Y(Z+1))]$$

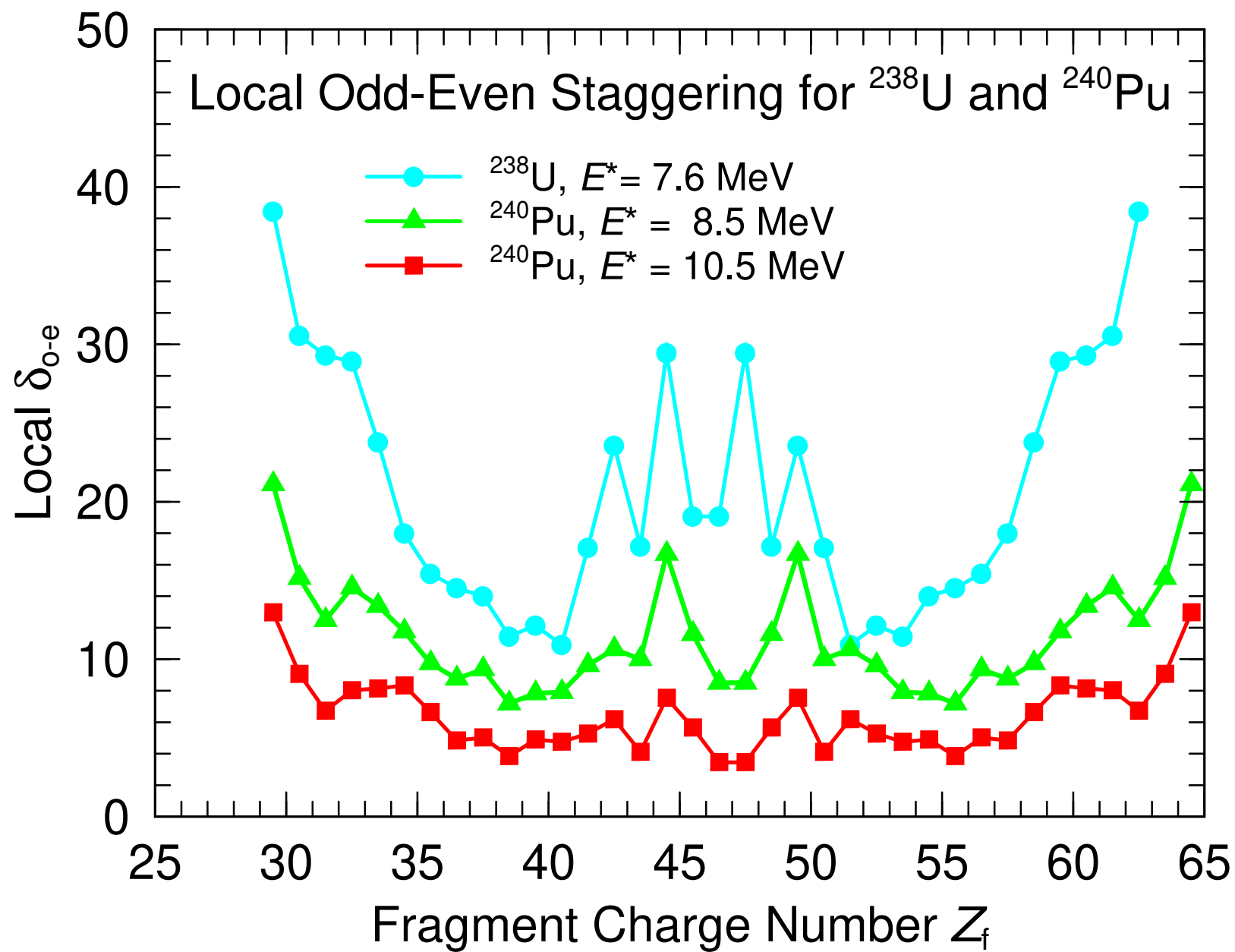
A global measure δ_{g-oe} of odd-even staggering in nuclear charge yields is defined as

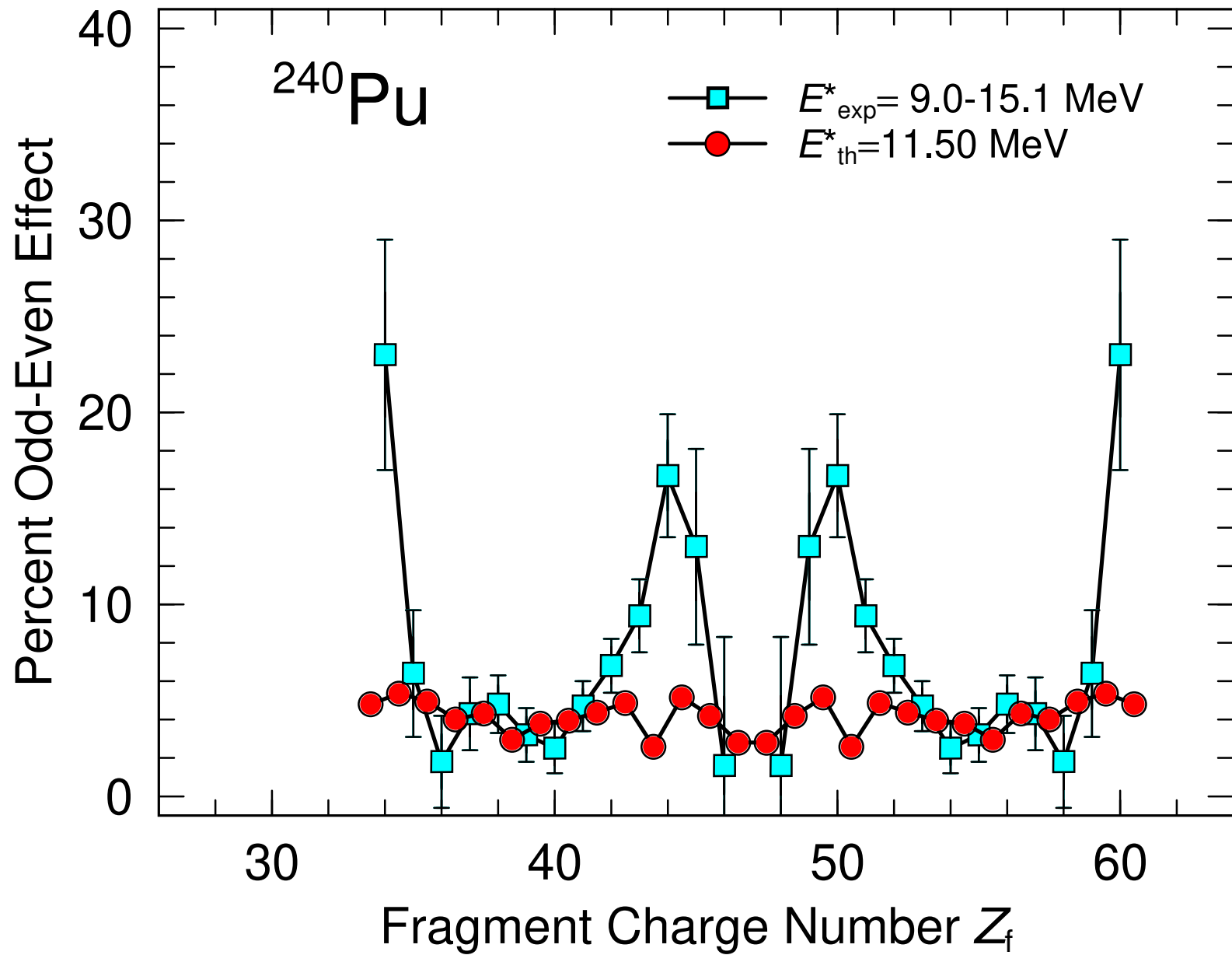
$$\delta_{g-oe} = 100 \times \frac{1}{\sum_Z Y(Z)} \sum_Z (-1)^Z Y(Z)$$

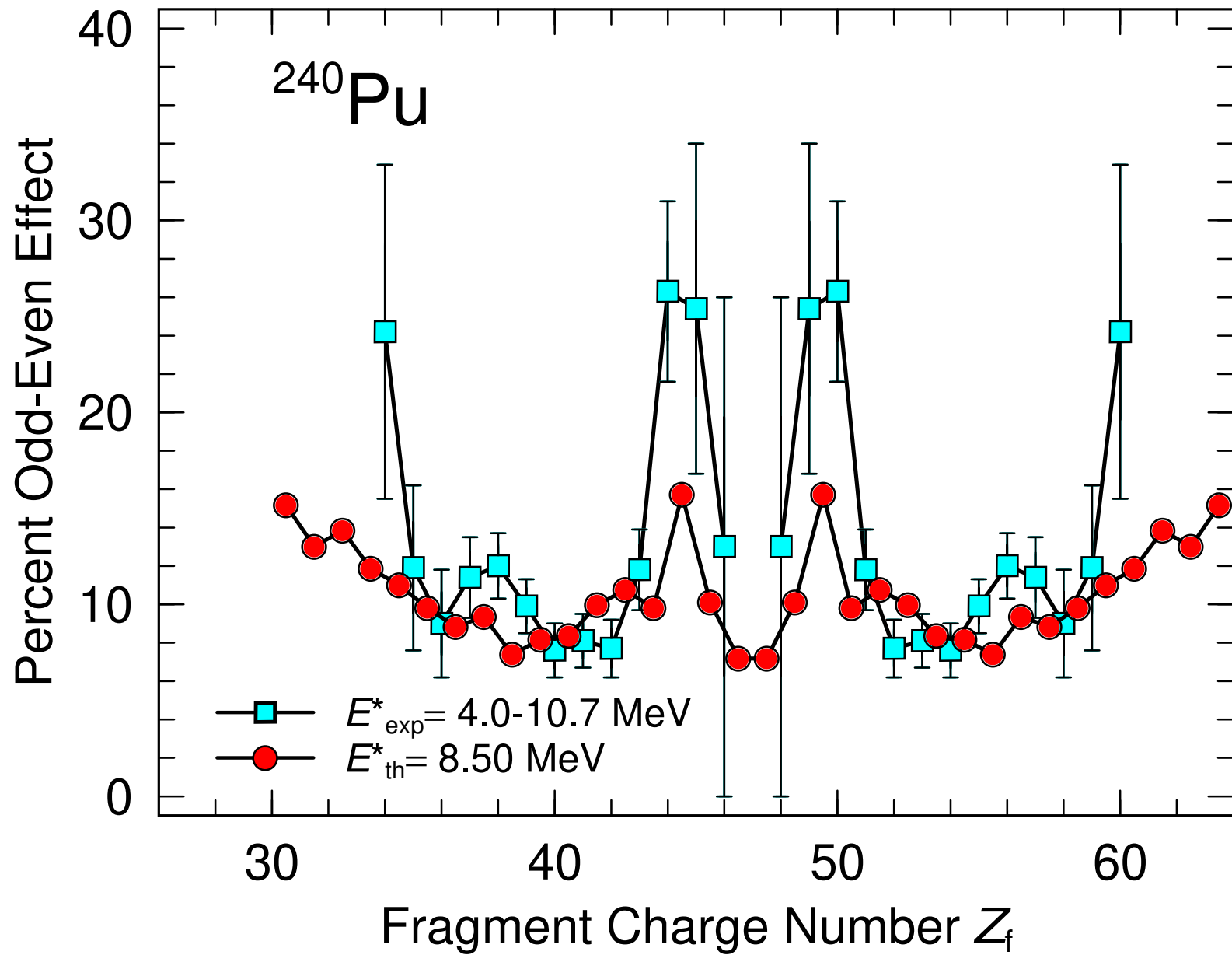


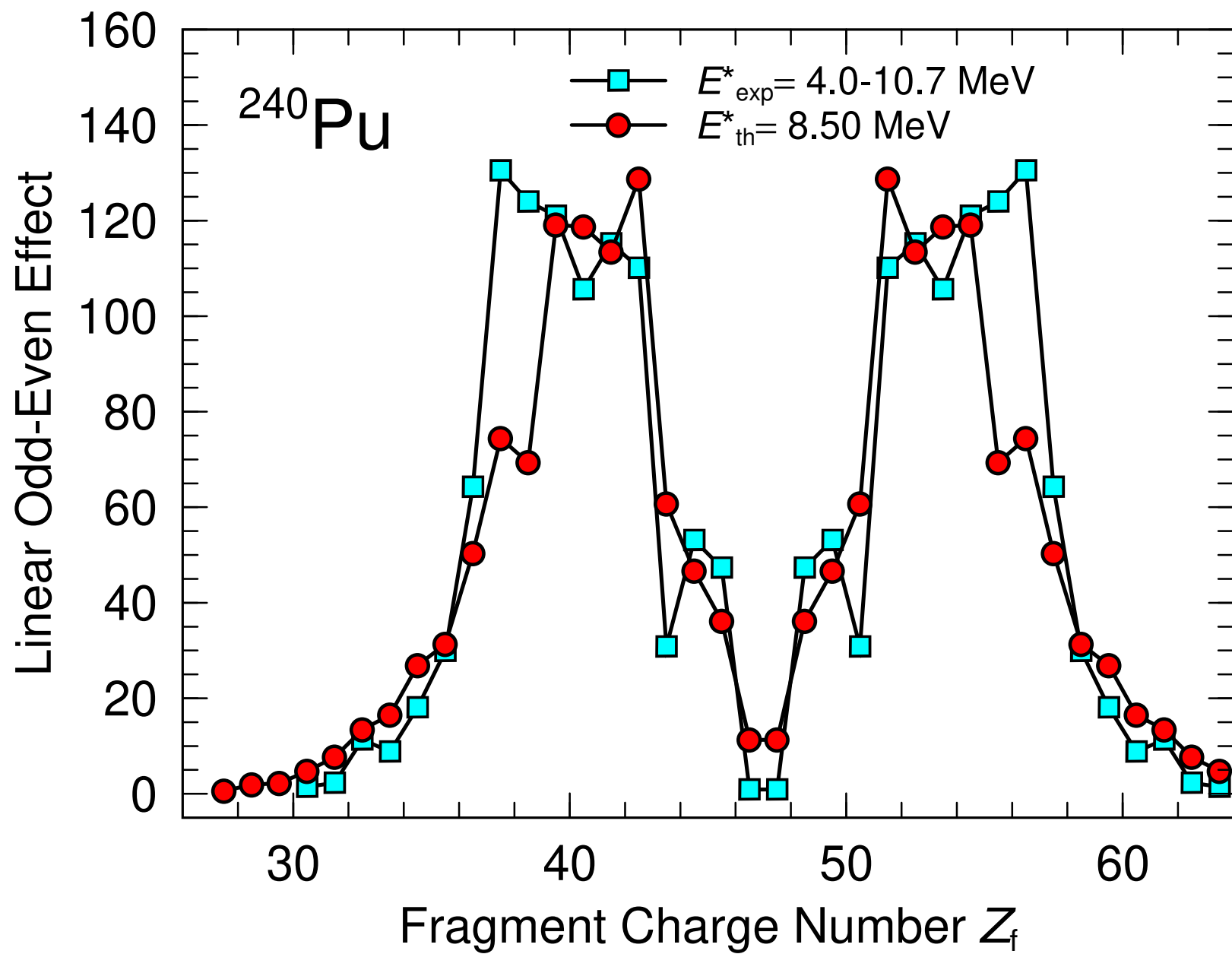


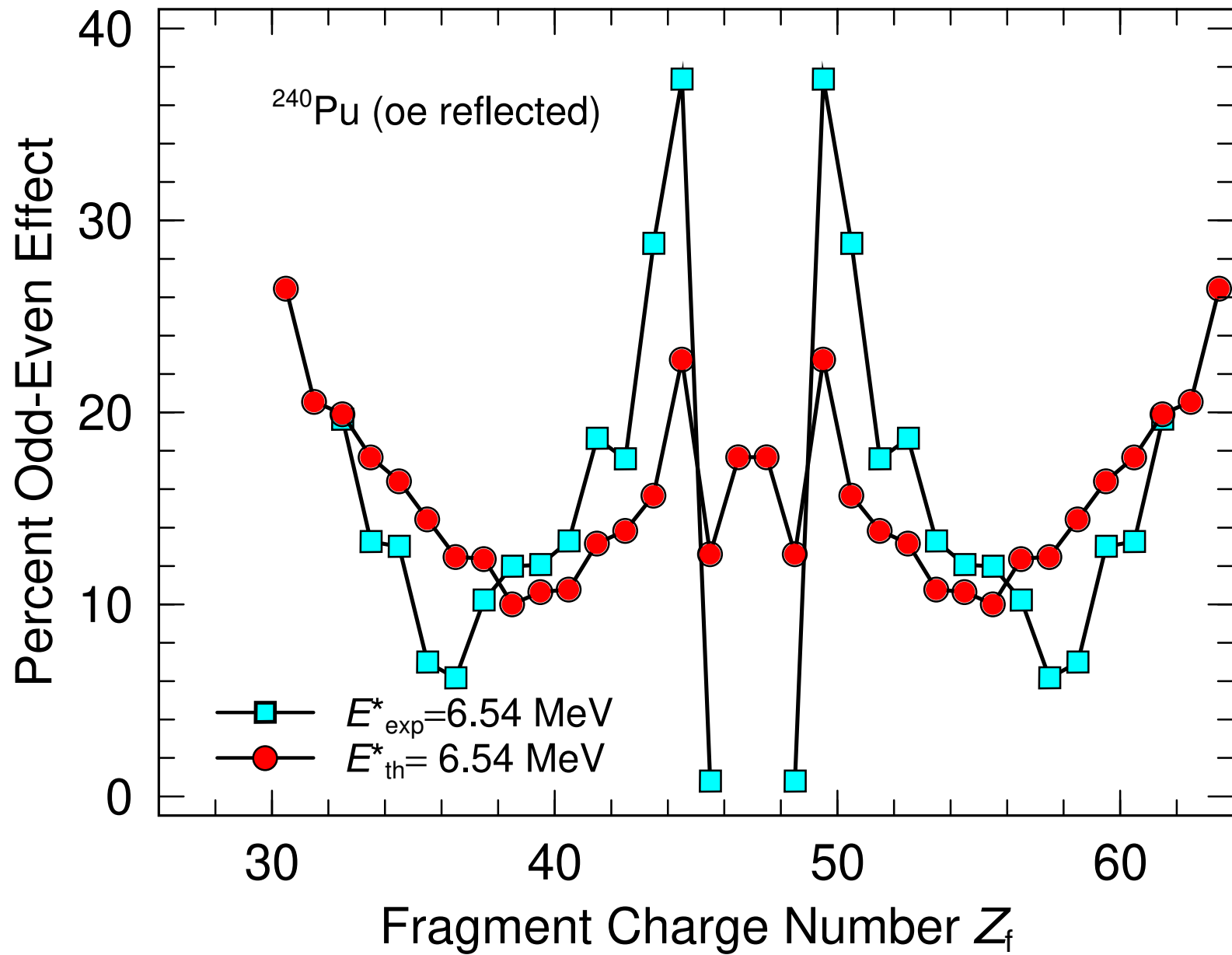


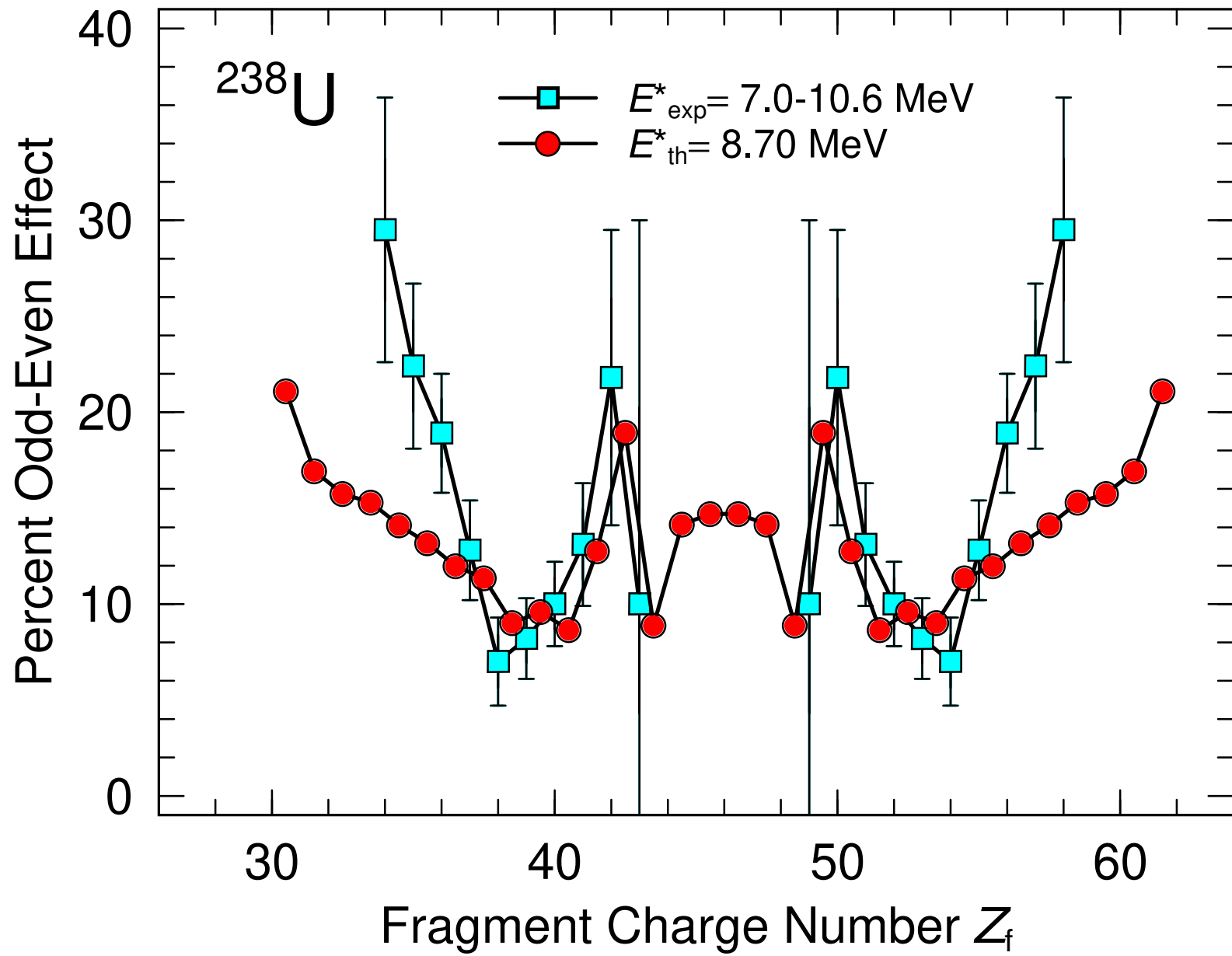


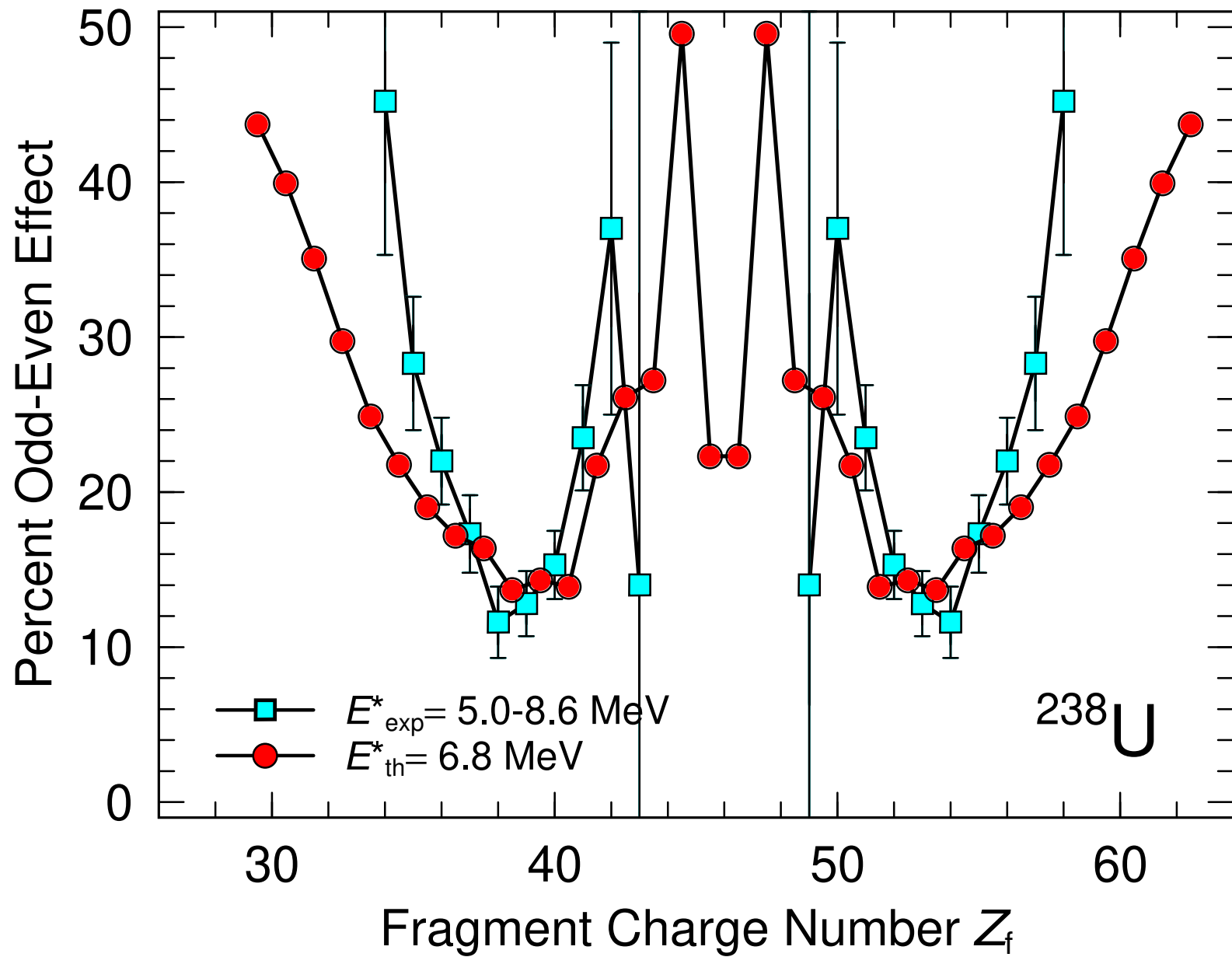















Measurement of mass and total kinetic energy distributions for the $^{12}\text{C} + ^{175}\text{Lu}$ systemSangeeta Dhuri ^{1,2}, K. Mahata ^{1,2,*}, A. Shrivastava,^{1,2} K. Ramachandran,¹ S. K. Pandit,¹ Vineet Kumar,¹ V. V. Parkar,^{1,2} P. C. Rout,^{1,2} A. Kumar,¹ Arati Chavan,³ Satbir Kaur,^{1,2} and T. Santhosh ^{1,2}¹Nuclear Physics Division, Bhabha Atomic Research Centre, Mumbai 400085, India²Homi Bhabha National Institute, Anushaktinagar, Mumbai 400094, India³Vivekanand Education Society's College of Arts, Science and Commerce, Mumbai 400071, India

(Received 17 May 2022; accepted 8 July 2022; published 21 July 2022)

Fission fragment mass and total kinetic energy (TKE) distributions were measured for $^{12}\text{C} + ^{175}\text{Lu}$ system at excitation energies down to 16.7 MeV above the saddle point. The overall mass and TKE distributions could be fitted with single Gaussian functions. The observed width of the mass and TKE distributions agree well with the systematics based on liquid drop (LD) behavior. The average TKE also shows parabolic dependence on fragment mass, as expected from LD behavior. Small contributions due to microscopic corrections from $Z \approx 38$ and 45 shells can be extracted, if the widths of the LD component are fixed from systematics. Contrary to the theoretical predictions of substantial contributions from microscopic corrections, dominance of liquid drop behavior was observed.

DOI: [10.1103/PhysRevC.106.014616](https://doi.org/10.1103/PhysRevC.106.014616)**I. INTRODUCTION**

Nuclear fission is one of the most intricate processes of nuclear decay, where a heavy nucleus splits into two or more lighter nuclei having similar masses, releasing large amount of energy. The fission process was explained using the liquid drop model (LDM), which considers the nucleus as an incompressible macroscopic liquid drop [1,2]. However, the LDM could not explain the predominant asymmetric mass split at low excitation energy in the actinide region. The incorporation of microscopic effects such as shell corrections to the macroscopic liquid drop (LD) paved the way to understanding the observed mass asymmetry [3]. The potential energy landscape with multiple valleys created by the microscopic corrections was found to strongly influence the characteristics, e.g., mass split, total kinetic energy (TKE), and neutron multiplicities in low energy fission of actinides. The concept of different fission modes, i.e., “superlong” (SL) symmetric fission mode and asymmetric “standard” fission modes ($S1$ and $S2$) was introduced [4].

Over the years, a vast knowledge base of fission of actinides has been created and is still being enriched experimentally as well as theoretically [5–7]. However, the low energy fission of preactinide nuclei remained less explored, as the increase in liquid drop fission barrier height with decreasing fissility drastically reduces fission probability at low energies. It also was expected that the liquid drop (symmetric) fission will dominate in the preactinide region. In 1980s, series of measurements were carried out by Itkis *et al.* [8–10] by bombarding p and α particles on stable preactinide targets. Symmetric fission was indeed found to dominate in this

region. It was demonstrated that the yields of asymmetric components ($S1$ and $S2$), which are very dominant in the actinide region, diminish with decreasing N and Z of the fissioning nuclei and vanish at ^{201}Tl . Flattening or a slight dip in the mass distribution around half the mass of the fissioning nucleus (A_{CN}) was also observed in most of the cases. It was interpreted in terms of positive shell corrections at $A_{CN}/2$ in contrast to negative shell corrections for $S1$ and $S2$. Later, the flattening of the mass distributions at $A_{CN}/2$ was attributed to two strongly deformed neutron shells in the nascent fragments with neutron numbers $N_1 \approx 52$ and $N_2 \approx 68$ [11].

Recent unexpected observation of almost exclusive asymmetric fission in neutron-deficient ^{180}Hg [12] at low energy has put the focus back on this region. From the liquid drop as well as spherical shell gaps perspective, splitting into two symmetric doubly magic ^{90}Zr fragments ($N = 50$, $Z = 40$) should have been the most favored. Several other measurements [13–23] have firmly established the presence of asymmetric fission in this region. However, it is still not clear what drives the asymmetry in fission of preactinides. Theoretical models based on different approaches, e.g., Brownian shape motion on the macroscopic-microscopic potential energy surface [24], the improved scission point model [25], and the time independent microscopic model [26], have interpreted these observations differently. The macroscopic-microscopic model [27,28] attributed this to the saddle asymmetry and predicted a region of asymmetry centered around ^{186}Pt . Calculations based on the microscopic energy density functional (EDF) framework [26,29] result in shell gaps at $N = 52$ – 56 and $Z = 34$ – 38 , 42 – 46 due to quadrupole-octupole correlations. A recent systematic study of the experimental results has demonstrated the dominance of proton shells ($Z \approx 36$) [29] in the light fragment in deciding the asymmetric split in the preactinide region, in contrast to

*Corresponding author: kmahata@barc.gov.in

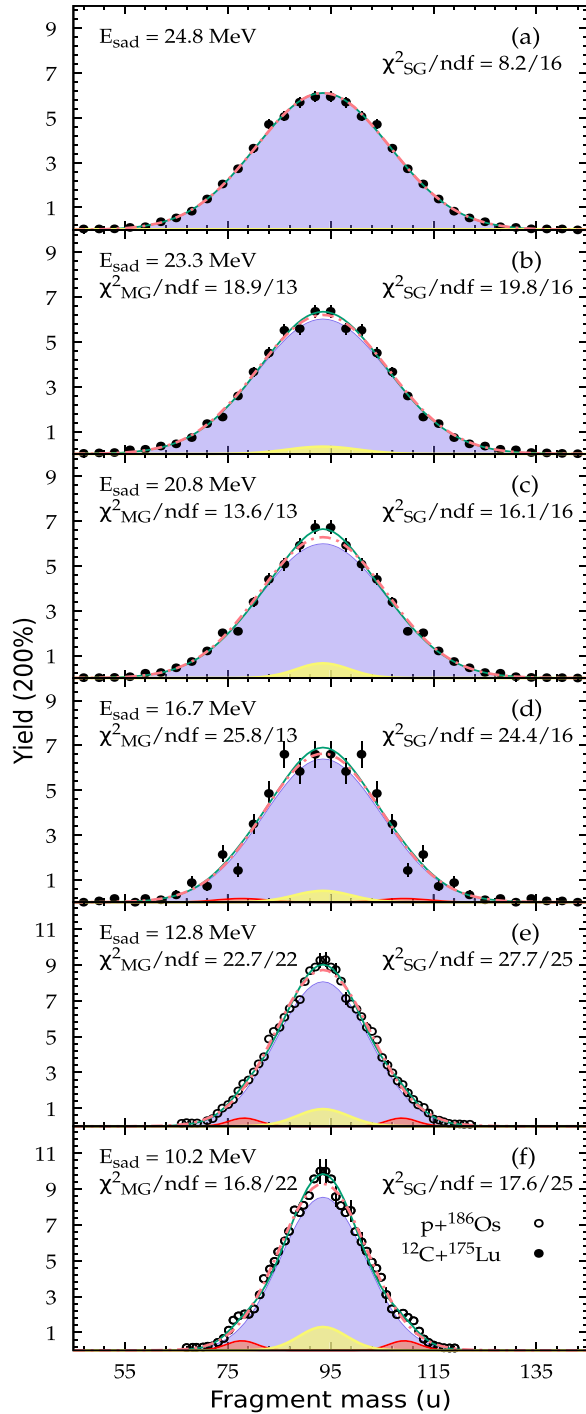


FIG. 3. The experimental mass distributions (a)–(d) for the $^{12}\text{C} + ^{175}\text{Lu}$ reaction from the present measurement (filled circles) and (e)–(f) for the $p + ^{186}\text{Os}$ reaction [10] (open circles) are plotted with increasing excitation energy at the saddle point (E_{sad}) from bottom to top panels. The solid lines show the multi-Gaussian (MG) fits to the data along with different fissioning modes corresponding to macroscopic liquid drop component (violet shaded region) and microscopic component due to $Z \approx 38$ (yellow shaded region) and $Z \approx 45$ (red shaded region) shells. The dot-dashed line is the single Gaussian (SG) fit to the data. The corresponding χ^2 and the number of degrees of freedom (ndf) are also mentioned.

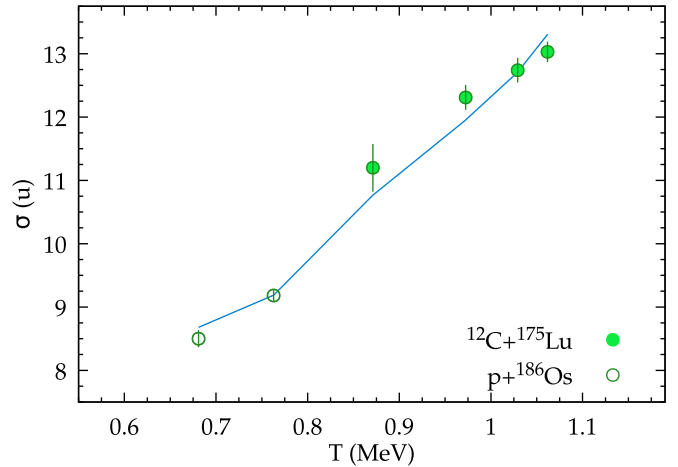
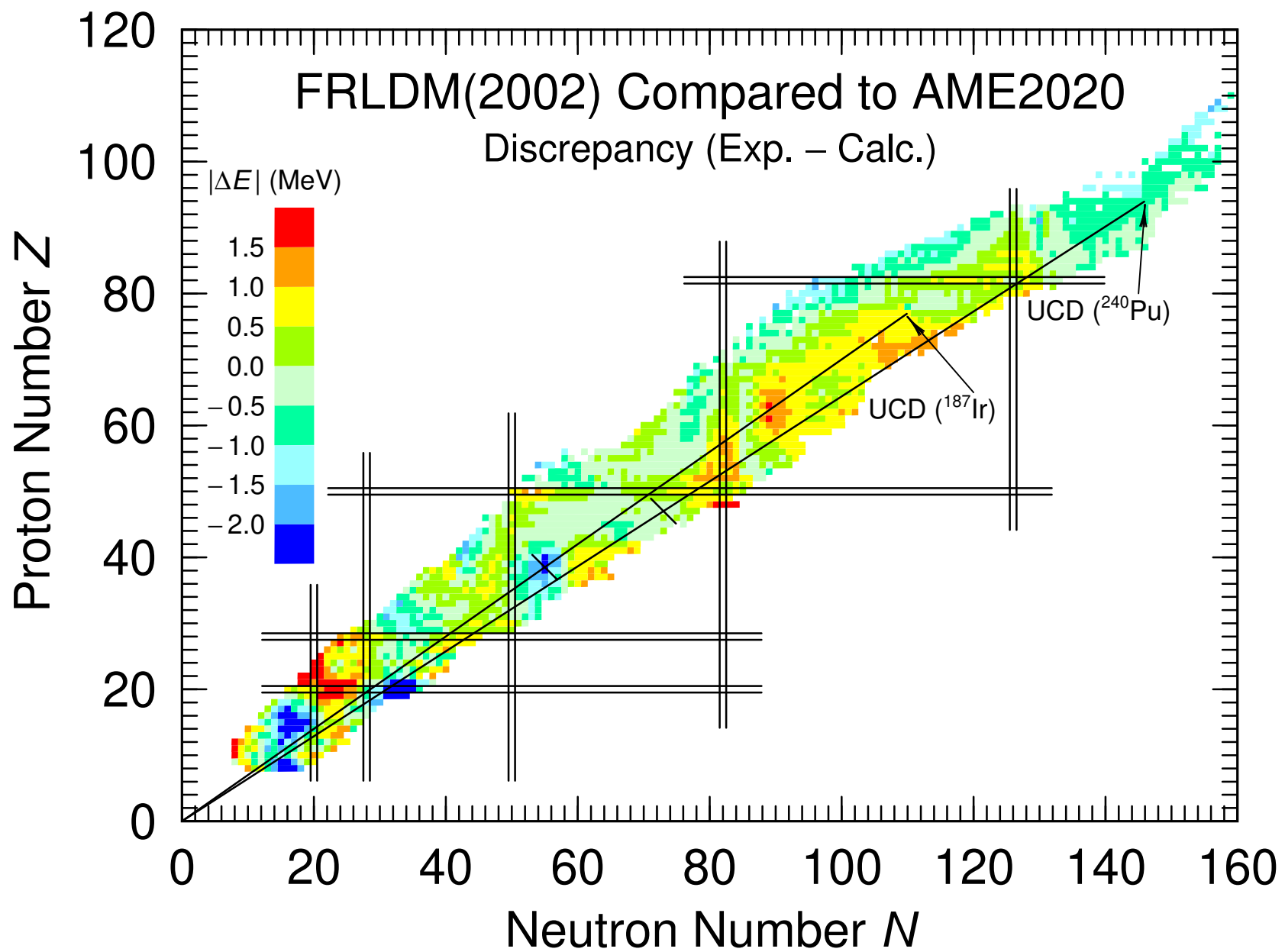


FIG. 4. The extracted mass widths from single Gaussian fits (σ_M) are plotted as a function of temperature at the saddle point (T) for present measurement $^{12}\text{C} + ^{175}\text{Lu}$ (filled circles) and $p + ^{186}\text{Os}$ [10] (open circles). The solid line is the description using Eq. (2).

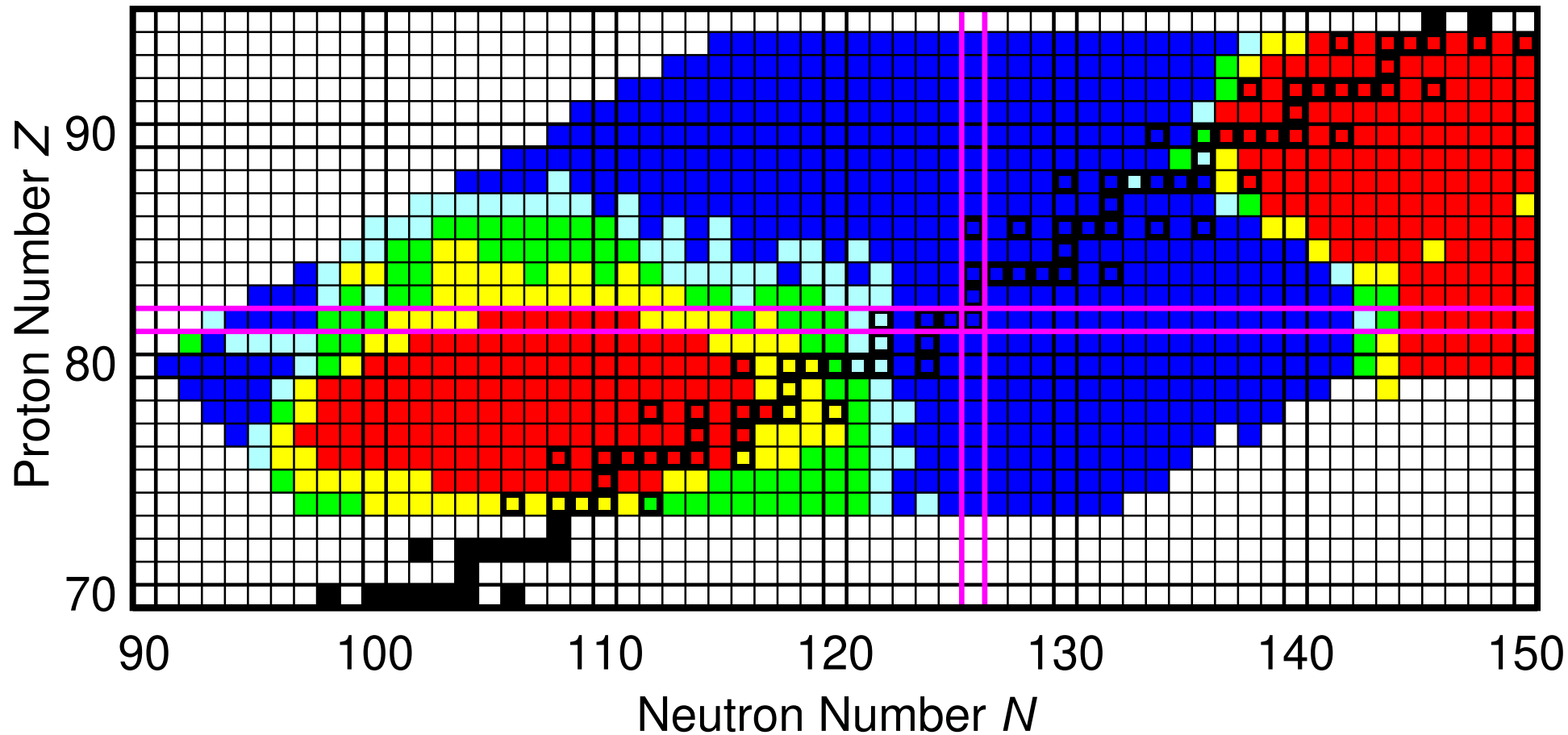
statistical relation [39]

$$\sigma_{MR}^2 = \lambda T + \kappa \langle \ell_{\text{fis}}^2 \rangle. \quad (2)$$

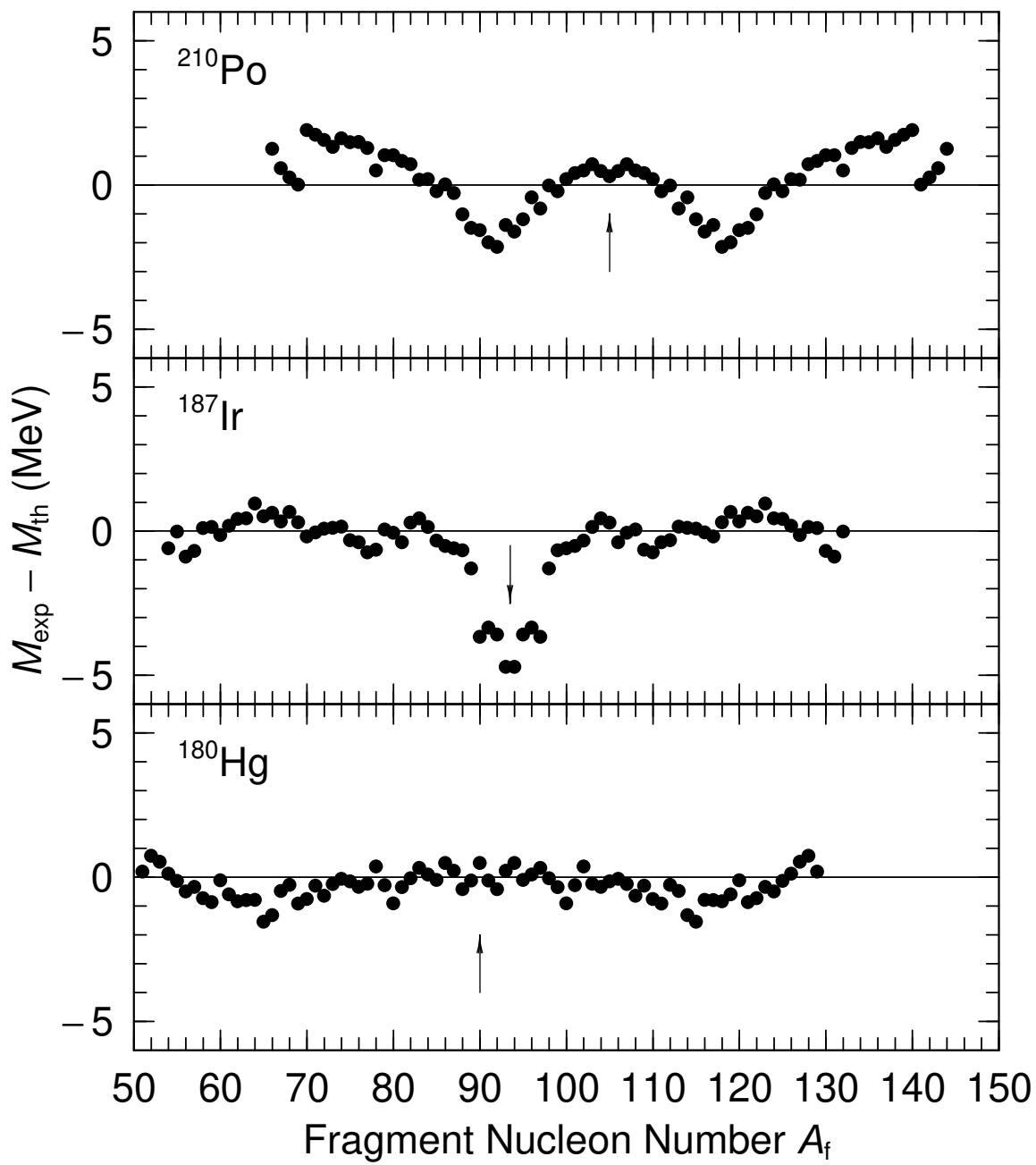
The temperature at the saddle (T) and the ℓ^2 average of the fissioning nuclei ($\langle \ell_{\text{fis}}^2 \rangle$) are tabulated in Table I along with other relevant quantities. The fusion ℓ distributions, calculated using the CCFULL code [40] after fitting the fusion excitation function for the $^{12}\text{C} + ^{175}\text{Lu}$ system [32], were used as an input for the statistical model calculations using the code PACE [41,42] to estimate the values of average angular momentum ($\langle \ell_{\text{fis}} \rangle$), average square angular momentum ($\langle \ell_{\text{fis}}^2 \rangle$), pre-fission neutron multiplicity (ν_{pre}), and average energy removed by pre-fission neutron emission (E_{eva}). The temperature at the saddle point was calculated as $T = \sqrt{E_{\text{sad}}/a}$ with $a = A/8.5$. The effective excitation energy of the fissioning nucleus at saddle is calculated as $E_{\text{sad}} = E_{CN}^* - B_{f,(\ell_{\text{fis}})} - \Delta E_{\text{eva}} - E_{\text{rot}}$. The average ℓ -dependent fission barrier heights $B_{f,(\ell_{\text{fis}})}$ are calculated using $B_{f,(\ell_{\text{fis}})} = B_{f,0} - \Delta B_{f,(\ell_{\text{fis}})}$, with $B_{f,0}$ the value of fission barrier height at zero angular momentum taken from Ref. [43]. The change in the fission barrier due to rotation (ΔB_f) and the rotational energy at the equilibrium deformation (E_{rot}) are taken from the rotating finite range model (RFRM) [44]. Though the entrance channel mass asymmetry parameters for $p + ^{186}\text{Os}$ (0.98) and the present system (0.87) are very different, they are much larger than the Businaro-Gallone critical mass asymmetry parameter ($\alpha_{BG} = 0.81$). Thus both systems are expected to exhibit characteristics of statistical decay of a fully equilibrated compound nucleus. As shown in Fig. 4, experimental mass widths for $p + ^{186}\text{Os}$ and the present system could be simultaneously fitted well using the statistical relation given in Eq. (2), indicating the absence of any significant entrance channel dependence. The resulting parameters are $\lambda = (3.12 \pm 0.12) \times 10^{-3}$ and $\kappa = (1.93 \pm 0.24) \times 10^{-6}$. These values are similar to the values obtained for nearby systems $^{16}\text{O} + ^{175}\text{Lu}$ [18] and $^{16}\text{O} + ^{186}\text{W}$ [45]. The extracted value of the stiffness



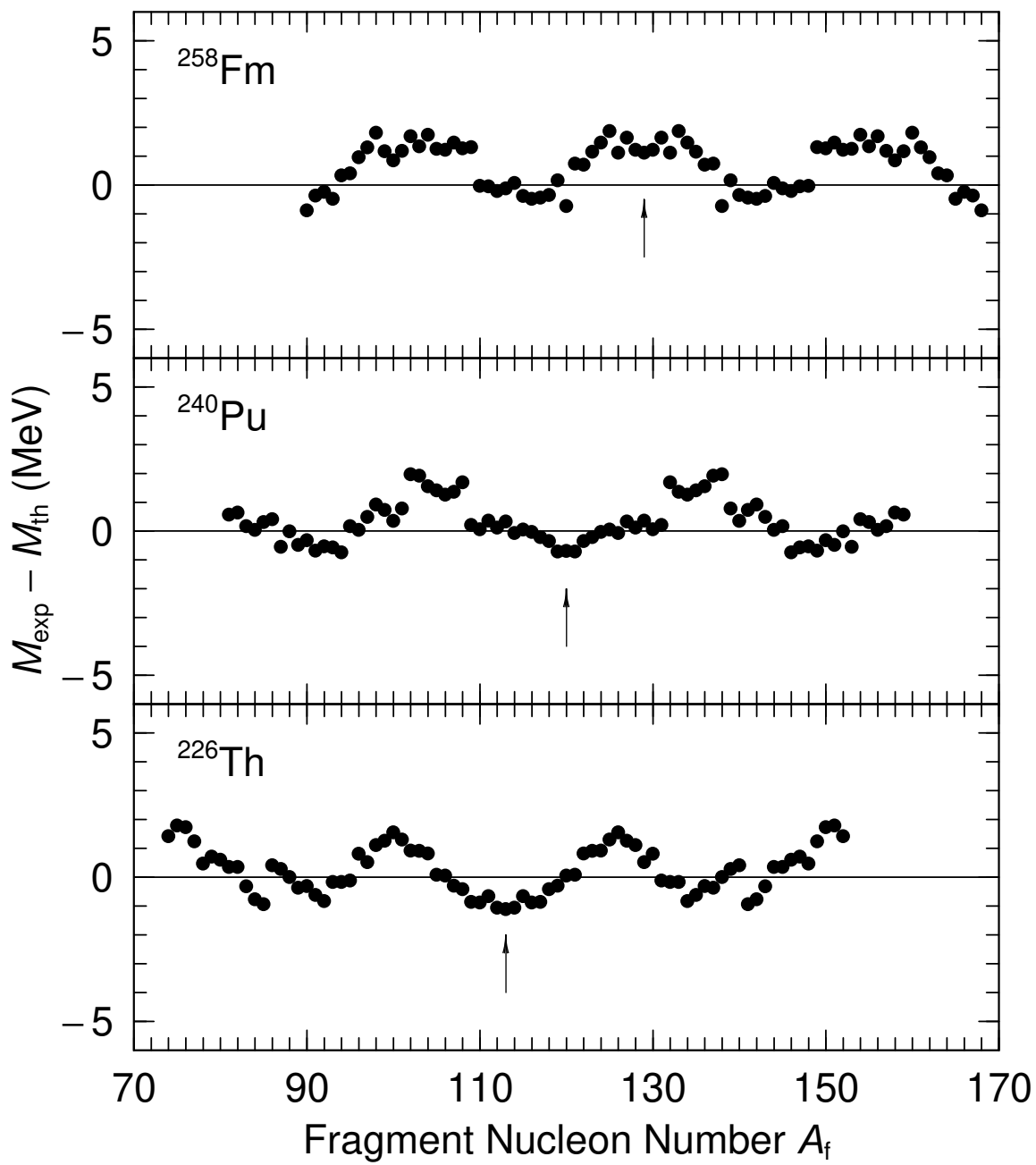
Fission-Fragment Symmetric-Yield to Peak-Yield Ratio



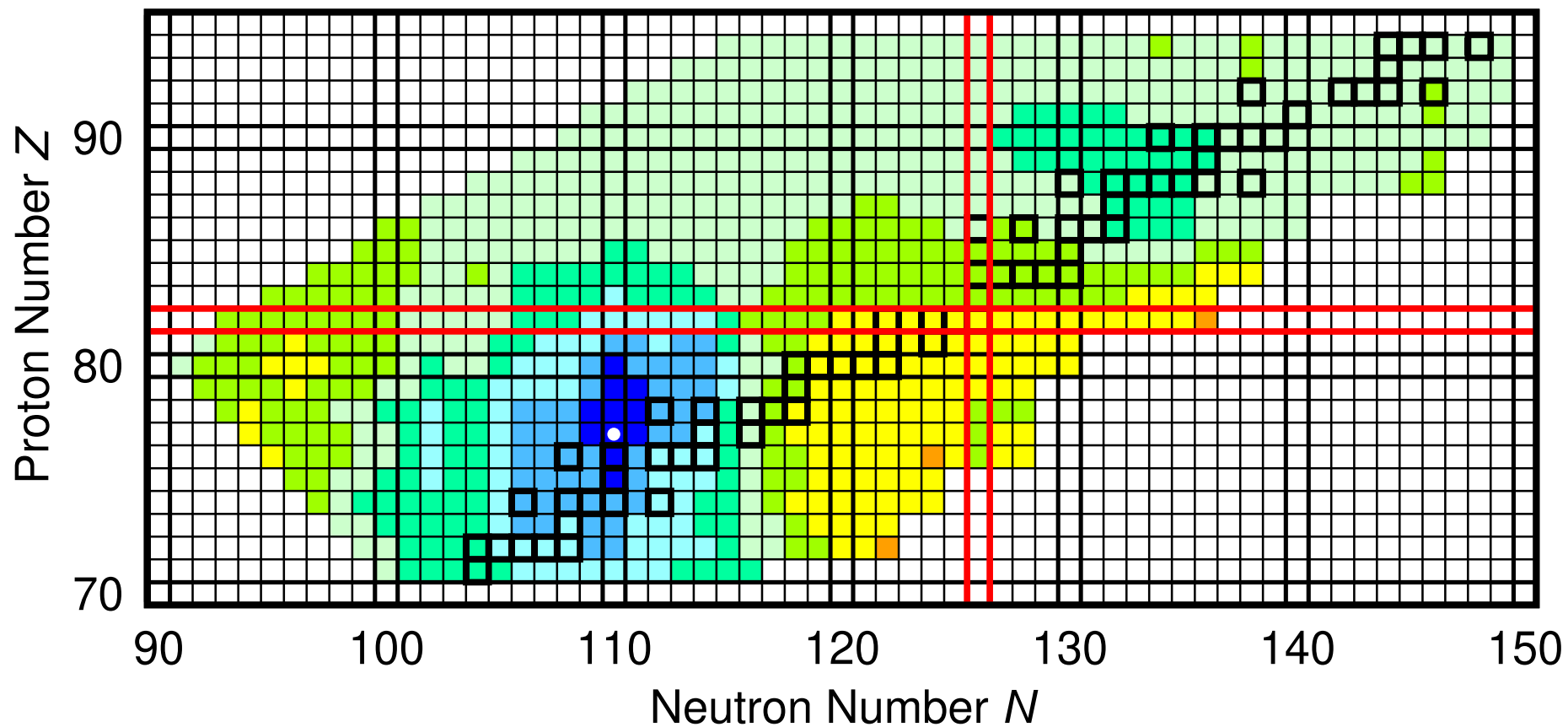
UCD Potential-Energy Mass Defect at Scission



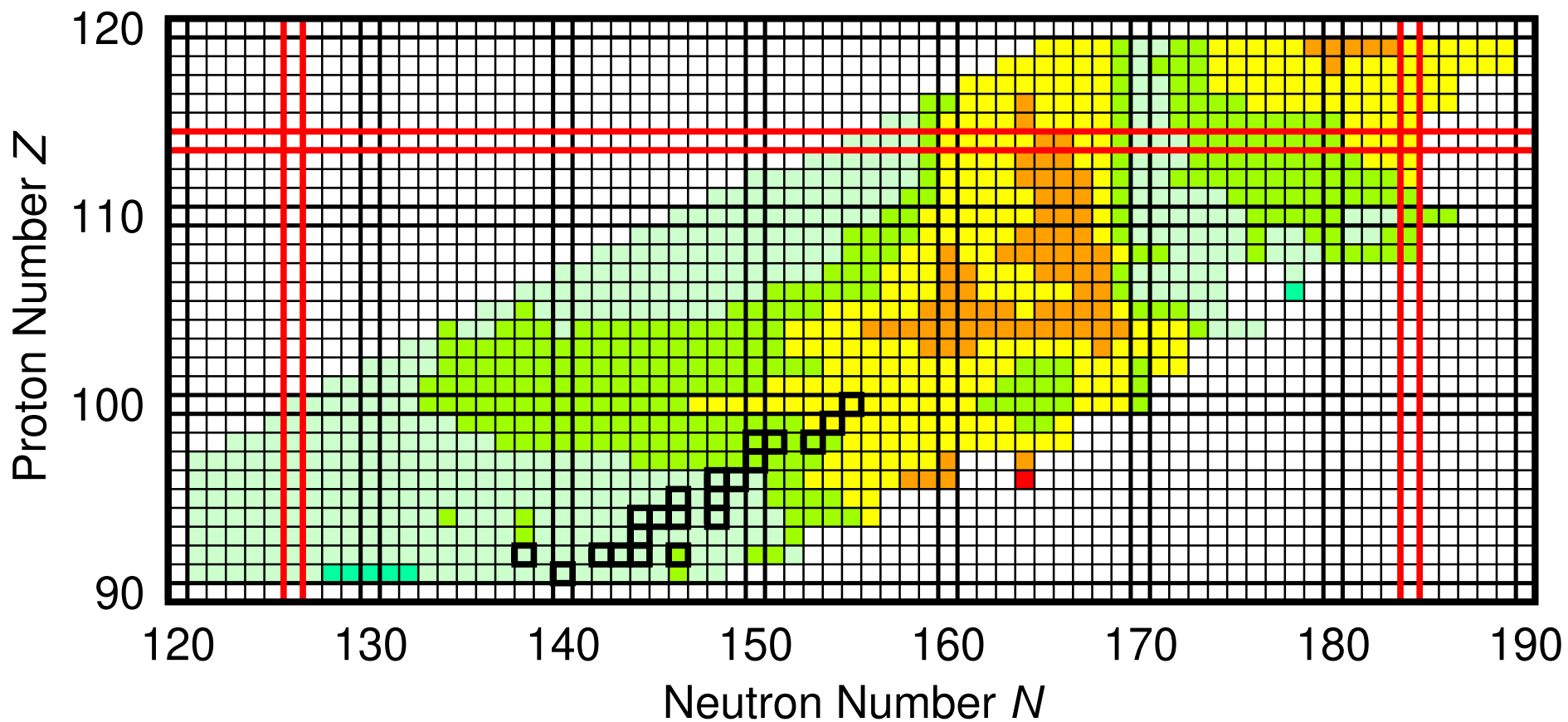
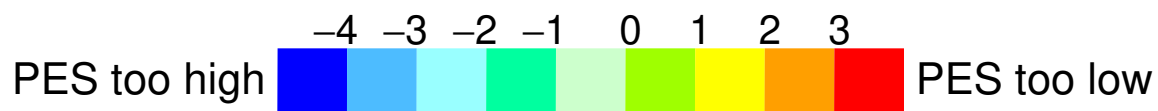
UCD Potential-Energy Mass Defect at Scission



Calculated PES Error for Symmetric Split



Calculated PES Error for Symmetric Split



List of publications relevant to Moller presentation 2024-10-31

FISSION-RELATED PUBLICATIONS

1. CALCULATED FISSION PROPERTIES OF THE HEAVIEST ELEMENTS,
P. Möller, J. R. Nix and W. J. Swiatecki
Nucl. Phys. **A469** (1987) 1
2. NEW DEVELOPMENTS IN THE CALCULATION OF HEAVY-ELEMENT FISSION BARRIERS,
P. Möller, J. R. Nix and W. J. Swiatecki
Nucl. Phys. **A492** (1989) 349-387
3. **TOPICAL REVIEW: STABILITY OF HEAVY AND SUPERHEAVY ELEMENTS**,
P. Möller and J. R. Nix
Journal of Physics G: Nuclear and Particle Physics, TOPICAL REVIEW, **20** (1994) 1681–1747
4. REALISTIC FISSION SADDLE-POINT SHAPES.
P. Möller and A. Iwamoto,
Phys. Rev. **C 61** (2000) 47602
5. TOPOLOGY OF FIVE-DIMENSIONAL, MILLION-GRID-POINT FISSION POTENTIAL-ENERGY SURFACES IN THE 3QS PARAMETERIZATION,
Peter Möller and Akira Iwamoto,
Proc. Conf on Nuclear Shapes and Motions, Santa Fe, New Mexico, Oct. 25–28 (1998)
ACTA PHYSICA HUNGARICA NEW SERIES-HEAVY ION PHYSICS, 10 pp. 241-251 1999
6. NUCLEAR FISSION MODES AND FRAGMENT MASS ASYMMETRIES IN A FIVE-DIMENSIONAL DEFORMATION SPACE, Peter Möller, David G. Madland, Arnold J. Sierk, and Akira Iwamoto,
Nature **409** (2001) 785–790
7. INTO THE FISSION VALLEY,
Peter Möller and Arnold J. Sierk,
Nature, **422** (2003) 485–486
8. FIVE-DIMENSIONAL FISSION-BARRIER CALCULATIONS FROM ^{70}Se TO ^{252}Cf ,
Peter Möller, Arnold J. Sierk, and Akira Iwamoto,
Phys. Rev. Lett. **92** (2004) 072501
9. HEAVY-ELEMENT FISSION-BARRIERS Peter Möller, Arnold J. Sierk, T. Ichikawa, A. Iwamoto, Ragnar Bengtsson, Henrik Uhrenholt, and Sven Åberg,
Phys. Rev. C **79** (2009) 064304 38 pages.
10. ORIGIN OF THE NARROW, SINGLE PEAK IN THE FISSION-FRAGMENT MASS DISTRIBUTION FOR ^{258}Fm , T. Ichikawa, A. Iwamoto, and P. Möller,
Phys. Rev. C **79** (2009) 014305
11. A NEW TYPE OF ASYMMETRIC FISSION IN PROTON-RICH NUCLEI
A.N. Andreyev, J. Elseviers, M. Huysse, P. Van Duppen, S. Antalic, A. Barzakh, N. Bree, T.E. Cocolios, V. F. Comas, J. Diriken, D. Fedorov, V. Fedosseev, S. Franchoo, J.A. Heredia, O. Ivanov, U. Köster, B. A. Marsh, K. Nishio, R.D. Page, N. Patronis, M. Seliverstov, I. Tsekhanovich, P. Van den Bergh, J. Van De Walle, M. Venhart, S. Vermote, M. Veselsky, C. Wagemans, T. Ichikawa, A. Iwamoto, P. Möller, and A.J. Sierk,
Phys. Rev. Lett. **105** (2010) 252502

12. BROWNIAN SHAPE MOTION ON FIVE-DIMENSIONAL POTENTIAL-ENERGY SURFACES:NUCLEAR FISSION-FRAGMENT MASS DISTRIBUTIONS J. Randrup and P. Möller, Phys. Rev. Lett. **106** (2011) 132503106
13. FISSION-FRAGMENT MASS DISTRIBUTIONS FROM STRONGLY DAMPED SHAPE EVOLUTION J. Randrup, P. Möller, and A. J. Sierk Phys. Rev. C **84** (2011) 034613
14. CALCULATED FISSION YIELDS OF NEUTRON-DEFICIENT MERCURY ISOTOPES, P. Möller, J. Randrup, and A. J. Sierk, Phys. Rev. C, **85** (2012) 024306
15. THE CONTRASTING FISSION POTENTIAL-ENERGY STRUCTURE OF ACTINIDES AND MERCURY ISOTOPES, Takatoshi Ichikawa, Akira Iwamoto, Peter Möller, and Arnold J. Sierk, Phys. Rev. C **86** (2012) 024610
16. CHARACTER AND PREVALENCE OF THIRD MINIMA IN ACTINIDE FISSION BARRIERS, Takatoshi Ichikawa, Peter Möller, and A. J. Sierk Phys. Rev. C **87** (2013) 054326,
17. ENERGY DEPENDENCE OF FISSION-FRAGMENT MASS DISTRIBUTIONS FROM STRONGLY DAMPED SHAPE EVOLUTION, Jørgen Randrup and Peter Möller, Phys. Rev. C **88** (2013) 064606,
18. FISSION-FRAGMENT CHARGE YIELDS: VARIATION OF ODD-EVEN STAGGERING WITH ELEMENT NUMBER, ENERGY, AND CHARGE ASYMMETRY, Peter Möller, Jørgen Randrup, Akira Iwamoto, and Takatoshi Ichikawa, Phys. Rev. C **90** (2014) 014601
19. CALCULATED FISSION-FRAGMENT YIELD SYSTEMATICS IN THE REGION $74 \leq Z \leq 94$ AND $90 \leq N \leq 150$, Peter Möller, Jørgen Randrup, Phys. Rev. C **91** (2015) 044316
20. FISSION BARRIERS AT THE END OF THE CHART OF THE NUCLIDES, Peter Möller, Arnold J. Sierk, Takatoshi Ichikawa, Akira Iwamoto, and Matthew Mumpower, Phys. Rev. C **91** (2015) 024310,
21. A METHOD TO CALCULATE FISSION-FRAGMENT YIELDS $Y(Z, N)$ VERSUS PROTON AND NEUTRON NUMBER IN THE BROWNIAN SHAPE-MOTION MODEL; APPLICATION TO CALCULATIONS OF U AND PU CHARGE YIELDS Peter Möller and Takatoshi Ichikawa, European Physics Journal A. **51** (2015) 173

22. EVOLUTION OF URANIUM FISSION-FRAGMENT CHARGE YIELDS WITH NEUTRON NUMBER
Peter Möller and Christelle Schmitt,
European Physics Journal A **53** (2017) 7
23. NUCLEAR SHAPE EVOLUTION BASED ON MICROSCOPIC LEVEL DENSITIES
D. E. Ward, B.G. Carlsson, T. Døssing, and P. Möller, J. Randrup, and S. Åberg
Physical Review C, **95** (2017) 024618
24. THE MICROSCOPIC MECHANISM BEHIND THE FISSION-BARRIER ASYMMETRY (II): THE RARE-EARTH REGION $50 < Z < 82$ AND $82 < N < 126$
T. Ichikawa, P Möller
Phys. Lett. B **789** (2019) 679–684
25. EXCITATION ENERGY PARTITION IN FISSION
M. Albertsson, B.G. Carlsson, T. Døssing, P. Möller, J. Randrup, S. Åberg
Phys. Lett. B **803** (2020) 135276
26. CALCULATED FISSION-FRAGMENT MASS YIELDS AND AVERAGE TOTAL KINETIC ENERGIES OF HEAVY AND SUPERHEAVY NUCLEI
M. Albertsson, B.G. Carlsson, T. Døssing, P. Möller, J. Randrup, S. Åberg
Eur. Phys. J. A **56**, (2020) 46
27. ON THE ISOTOPIC COMPOSITION OF FISSION FRAGMENTS
C. Schmitt and P. Möller,
Phys. Lett. B **812** (2021) 136017
28. CORRELATION STUDIES OF FISSION FRAGMENT NEUTRON MULTIPLICITIES
M. Albertsson, B. G. Carlsson, T. Døssing, P. Möller, J. Randrup, S. Åberg
Phys. Rev. C **103**, (2021) 014609
29. DETAILED MODELING OF ODD-EVEN STAGGERING IN FISSION-FRAGMENT CHARGE DISTRIBUTIONS
Peter Möller and Christelle Schmitt,
European Physics Journal A **60:27** (2024)